

Shear Degradation of Vinylidene Chloride Copolymers

S. R. BETSO,¹ J. A. BERDASCO,¹ M. F. DEBNEY,¹ G. L. MURPHY,¹ N. P. ROME,¹
S. G. RICHARDS,¹ and B. A. HOWELL^{2,*}

¹Barrier Resins and Fabrication Research, Michigan Research and Development, The Dow Chemical Company, Midland, Michigan 48674; ²Department of Chemistry and Center for Applications in Polymer Science, Central Michigan University, Mt. Pleasant, Michigan 48859

SYNOPSIS

Thermally induced dehydrochlorination is a well-established and prominent degradation mode for vinylidene chloride copolymers. During extrusion, other processes may represent significant degradation pathways. Under shear in air, both oxidative chain-scission and cross-linking are prominent processes for both vinylidene chloride/vinyl chloride and vinylidene chloride/methyl acrylate copolymers. Both processes are dependent upon shear rate and temperature. The shear-stress dependency can be modeled by a kinetic expression that incorporates shear stress into the Arrhenius preexponential factor. Vinylidene chloride/methyl acrylate copolymers appear to be somewhat more susceptible to oxidative chain-scission than are comparable vinylidene chloride/vinyl chloride copolymers, presumably because of a rapid oxidative attack at exposed methyl acrylate units. Shear-induced degradation of these materials in air is characterized by early predominant chain-scission with cross-linking assuming a greater importance as a function of time. Degradation under shear in a nonoxidative environment is a much simpler process—oxidative chain-scission is suppressed and cross-linking is very similar to that observed in air.

© 1994 John Wiley & Sons, Inc.

INTRODUCTION

Vinylidene chloride copolymers are perhaps some of the most effective oxygen and moisture barrier resins available today for food packaging.^{1,2} The use of these materials requires that they be formulated and stabilized to minimize decomposition during the extrusion process. Proper formulation and stabilization requires an understanding of the decomposition processes that occur during extrusion. It is to this end that this work was undertaken.

Vinylidene chloride homopolymer is an exceptional barrier resin. This homopolymer, however, is thermally unstable and undergoes rapid dehydrochlorination when heated to its melting point ($\sim 200^\circ\text{C}$), making it unsuitable as an extrusion resin. Copolymers of vinylidene chloride and vinyl chloride or methyl acrylate, however, lack this functional defect and are extrudable when properly for-

mulated and stabilized. Previous work on the decomposition processes of vinylidene chloride copolymers has focused on thermal, nonshear-related processes (see Howell et al.³⁻⁵). Copolymers of vinylidene chloride are often used for studies of the degradation processes.⁴

The thermal degradation of poly(vinylidene chloride) homopolymer and copolymers occurs in two distinct steps: The first step is a chain-process dehydrochlorination that generates a polychloroethylene moiety. The polyene sequences subsequently cross-link via a Diels-Alder-type condensation. The second step is the final dehydrochlorination of a highly cross-linked network that leads to the formation of elemental carbon.² These processes have been extensively studied using thermogravimetric techniques⁶ and HCl-evolution monitoring.⁷

All the above work is excellent in elucidating the thermal decomposition mechanisms of vinylidene chloride copolymers but does not address the effect of shear on these processes. Shear can affect the thermal degradation process in a variety of ways: It may have no impact on any of the processes; it may

* To whom correspondence should be addressed.

accelerate some or all of the processes; it may decelerate some or all of the processes; or it may affect some processes and not others.

Assuming that shear or, more correctly, shear stress affects the thermal decomposition processes, its effects can be manifest as (1) an increase in the temperature of the system by viscous heat generation, (2) a change in the rate of decomposition by changing the activation energy of reaction, and (3) a change in the rate of decomposition by changing the Arrhenius preexponential factor. Shear heating will simply thermally accelerate any decomposition reaction.

Shear can raise the ground-state energies of polymeric reactants and reduce the energy needed to overcome the activation barrier for reaction. This mechanism was postulated by Zhurkov et al.,^{8,9} where the activation energy of reaction (E^*) took the form

$$E^* = E_A - a\sigma \quad (1)$$

where E^* is the effective activation energy; E_A , the nonstress-related activation energy; a , the activation reaction volume; and σ , the mechanical stress. This functionality was found empirically to be applicable to stressed polyethylene and isotactic polypropylene by Korsukov et al.¹⁰

That shear stress would affect the Arrhenius preexponential factor is not obvious until it is recalled that the preexponential factor contains an entropy of activation component.¹¹ Under isothermal conditions, it can be demonstrated that the viscous energy dissipation modifies the entropy of the system. This relationship can be derived as follows: Recall that

$$\frac{dE}{dt} = \tau\dot{\gamma} \quad (2)$$

where dE/dt is the rate of viscous energy dissipation per unit volume; τ , the shear stress; and $\dot{\gamma}$, the shear rate. At constant temperature (T), the viscous energy dissipation components are

$$\left(\frac{dE}{dt}\right)_T = \left(\frac{dH}{dt}\right)_T - T\left(\frac{dS}{dt}\right)_T \quad (3)$$

where dH/dt is the rate of enthalpy change due to viscous energy dissipation, and dS/dt , the rate of entropy change due to viscous energy dissipation, but

$$\left(\frac{dH}{dt}\right)_T = 0 \quad (4)$$

therefore,

$$\left(\frac{dS}{dt}\right)_T = -\frac{1}{T}\tau\dot{\gamma}. \quad (5)$$

Integrating eq. (5) at constant $\dot{\gamma}$ yields

$$S_{T,\dot{\gamma}} = -\frac{1}{T}\tau\dot{\gamma} \quad (6)$$

Shear stress, then, can affect the entropy of a system and manifest this change in the Arrhenius preexponential factor. Pohl et al.^{12,13} observed this effect for the chain-scission of polyisobutylene as

$$db/dt = \dot{\gamma}^{1.3}k \exp(11,000/RT) \quad (7)$$

where db/dt is the rate of bond breakage; k , the rate constant; and R , a gas constant.

There are many thermal decomposition processes that can be monitored for vinylidene chloride copolymers under shear. The focus of this study was those processes that affect the molecular weight of the resin, specifically, chain-scission and cross-linking.

This report demonstrates that shear stress accelerates both chain-scission and cross-linking in vinylidene chloride copolymers and that the shear-stress dependency can be modeled by a kinetic expression that incorporates shear stress into the Arrhenius preexponential factor, specifically as

$$A' = A\tau^a$$

where A' is the preexponential factor; A , the non-shear component of the preexponential factor; and a , a constant.

EXPERIMENTAL

Four suspension polymerized resins were prepared for this study: three vinylidene chloride (VDC)/vinyl chloride (VC) copolymers, and one vinylidene chloride/methyl acrylate (MA) copolymer:

VDC/VC-1: ~ 15 wt % VC, $M_n \simeq 37,000$, $M_w \simeq 97,000$, $M_z \simeq 182,000$

VDC/VC-2: ~ 15 wt % VC, $M_n \simeq 38,000$, $M_w \simeq 94,000$, $M_z \simeq 174,000$

VDC/VC-3: ~ 15 wt % VC, $M_n \simeq 50,000$, $M_w \simeq 127,000$, $M_z \simeq 229,000$

VDC/MA-1: ~ 6 wt % MA, $M_n \simeq 47,000$, $M_w \simeq 103,000$, $M_z \simeq 170,000$

Oven Aging

All samples were thermally aged at 150°C in a Napco Model 5851 Vacuum Oven (Napco Scientific Co.) equipped with a gas inlet and a gas outlet. Prepurified nitrogen gas or prepurified air purged the oven at a rate of ~ 50 cc/min during the thermal aging studies.

Temperature accuracy was assured by calibrating an Omega Pyrometer (Omega Engineering, Inc.) against a standardized mercury thermometer at 100°C and using the pyrometer to measure the temperature variance across the sample tray in the oven. During the thermal aging, the maximum temperature variance was $150 \pm 2^\circ\text{C}$. The maximum temperature variance across the sample tray was $\pm 1^\circ\text{C}$.

Shear Degradation

All resins were thermally degraded under shear in a Brabender Plasti-Corder torque rheometer equipped with a Model R.-E-0-6, Type GT421, S.B., mixing head with stainless-steel roller blades; the mixing head was oil-heated.

A typical procedure is as follows: The Brabender mixing head was heated to the desired temperature and the measuring head cleaned, at least three times, with Geon 87321 WHT 124 poly(vinyl chloride) (PVC) pellets (B. F. Goodrich, Chemical Group). The rotor blades were set to the desired rotation speed (rpm), the sample chamber purged with the desired atmosphere (1–2 min for nitrogen at > 50 cm³/min, 0 min for air, because with air the sample chamber was left open to the air atmosphere) and 60.0 g of resin rapidly added to the sample chamber. When the degradation atmosphere was nitrogen, the sample was added through a hopper feeder, the plunger of the hopper feeder was modified to allow ingress and egress of nitrogen gas at ~ 25 – 50 cm³/min, and the plunger was kept slightly above the molten polymer during the complete course of the experiment. When air was the degradation atmosphere, the sample was added directly to the sample chamber, and the sample chamber was left open to the air atmosphere during the complete course of the experiment. Torque (5000 m-g [meter-grams] full-scale) was plotted continuously as a function of time. The mixing head temperature and polymer

melt temperature were monitored and recorded at 5 min intervals with an Omega Model RD2030 recorder (Omega Engineering, Inc.) equipped with digital thermocouple display (this unit was calibrated to be accurate to $\pm 1^\circ\text{C}$ in the 150–250°C temperature range). At the end of the experiment (the feeder hopper and plunger were removed, if necessary), the molten cross-linked resin was quenched with water until enough melt strength was achieved to easily remove the resin from the mixing chamber. The blades and chamber were meticulously mechanically cleaned with brass wire gauze and brushes to remove all traces of decomposed resin. The system was reassembled and purged at least twice with Geon PVC pellets to complete the cleaning. The complete procedure was repeated, as appropriate, on a new sample.

The cleaning procedure outlined should do more than just clean the mixing assembly of unwanted polymer; it should passivate the stainless-steel metal surfaces. These passivated metal surfaces should be less susceptible to corrosion by hydrogen chloride and, thus, subsequent generation of iron and other Lewis acid metal chlorides should be minimized. It is believed that any contributions from the mixing chamber corrosion products are negligible in these studies and, if existent, are constant and do not represent an unknown, unaccounted variable.

It is very important to realize that for the unit used in this study the drive rotor blade rotates three revolutions (S_D) for every two revolutions (S_S) of the slave rotor blade and that the unit tachometer displays the revolutions per minute (rpm) of the drive blade. The average shear rate ($\dot{\gamma}$) that the resin sample experiences is a weighted-average of the shear rates of the drive and slave rotor blades.

Sample Gathering

During the course of the shear degradation studies in air, it was necessary to remove a resin aliquot for molecular weight analysis. The procedure used was as follows: When appropriate, normally at 5 min intervals, the rotation of the rotor blades was momentarily ceased and an ~ 0.2 g resin aliquot was removed with chromium-coated flat-faced pliers. Immediately after aliquot removal, the rotation of the blades was started again; this whole procedure normally took no more than ~ 5 s. Typically, ~ 5 – 12 aliquots were collected, representing an ~ 1.0 – 2.4 g resin from a 60 g sample. After all the aliquots were collected, they were stored at $\sim 5^\circ\text{C}$ until they were analyzed.

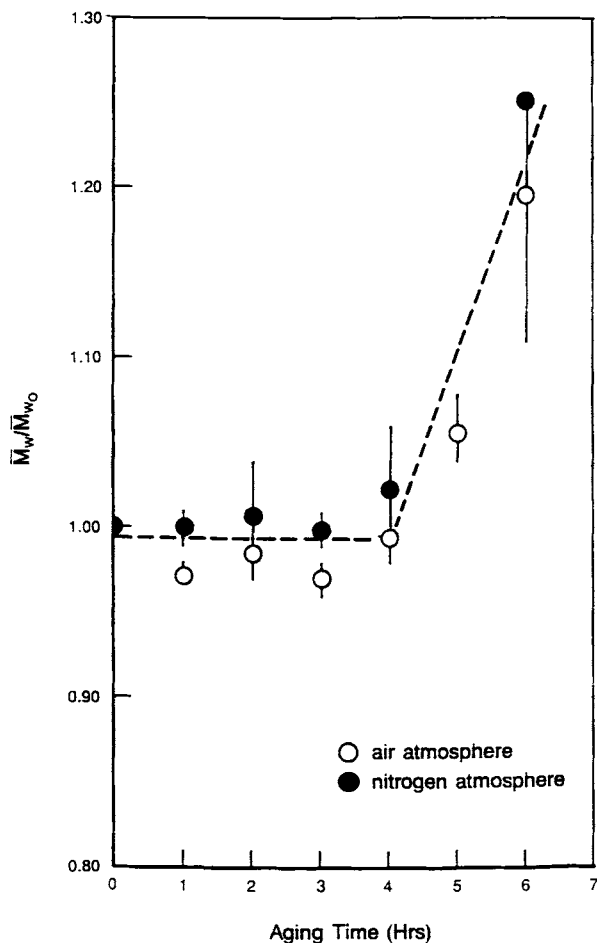


Figure 1 Normalized weight-average molecular weight data for VDC/VC-2 resin aged at 150°C.

Molecular Weight Measurements

Molecular weights and molecular weight distributions were determined by size exclusion chromatography (SEC) using columns calibrated with STYRON 1683 polystyrene resin.

RESULTS AND DISCUSSION

Quiescent Degradation

Shear can cause chain scission or cross-linking directly or it can simply accelerate thermal processes that lead to the same end. To determine if chain scission and cross-linking in VDC copolymers can result from thermal processes alone, it was necessary to study the degradation of these resins in the absence of shear. To this end, two resins, VDC/VC-1 and VDC/MA-1, were thermally aged at 150°C in nitrogen and in air; the results of these processes

on the weight-average molecular weight (M_w) of these resins are shown in Figures 1 and 2, respectively.

A thermal aging temperature of 150°C was chosen because it is a temperature hot enough to allow some melting of the low melting fractions of the polymers, but not complete melting; the resin beads remain intact and separated after ~ 6 h at this temperature, and this temperature is high enough to allow rapid, easily measurable dehydrochlorination to occur in a reasonable (hours) time. At 150°C, the weight loss for the VDC/VC-1 resin was replicately measured to be 1.05%, and 1.11% after 5.50 h under an air atmosphere.

The VDC copolymers are semicrystalline. At 150°C, the VDC/MA-1 and VDC/VC-1 copolymers consist of two phases: amorphous and crystalline. The amorphous phase is flexible and semipermeable to gases. The crystal phase is rigid and impermeable to gases. When a semicrystalline VDC copolymer is

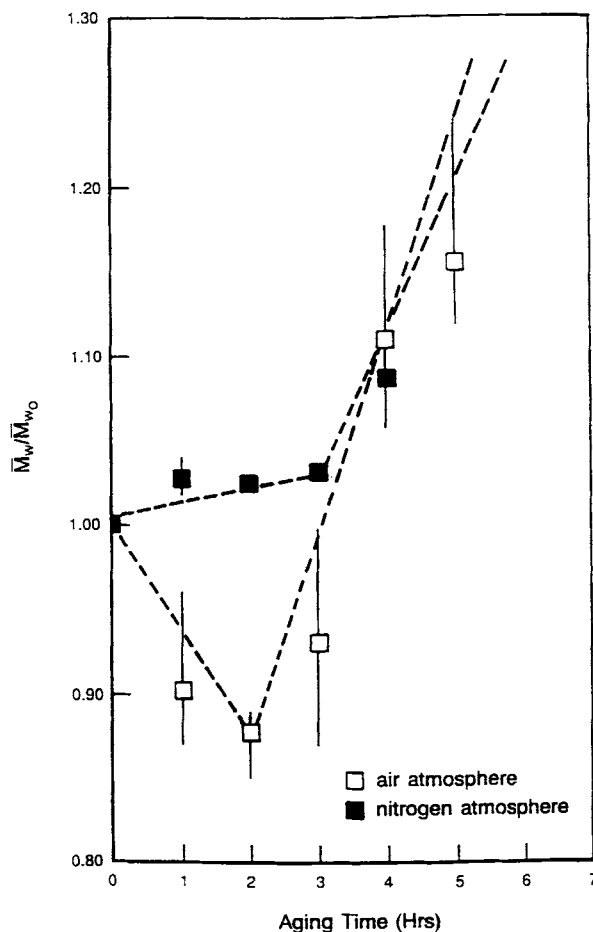


Figure 2 Normalized weight-average molecular weight data for VDC/MA-1 resin aged at 150°C.

thermally degraded, dehydrochlorination occurs equally in both phases. Oxidative degradation initially occurs only in the amorphous phase or on crystallite surfaces, as does cross-linking. As dehydrochlorination proceeds, the integrity of the crystal structure is destroyed, allowing chain movement and gas penetration; at this time, oxidative degradation and cross-linking can occur in this phase.¹⁴ This is illustrated in Figures 1 and 2. The weight-average molecular weight data for the VDC/VC-1 resin reflect no apparent cross-linking until ~ 4 h, then rapid cross-linking. After ~ 4 h, it appears as if enough crystalline structure has been destroyed to allow sufficient chain movement for cross-linking. Since the crystal is impervious to gases, this effect is the same in both atmospheres. For the VDC/VC-1 system, it appears as if oxidative chain-scission is not extensive enough to be detected by the weight-average molecular weight data.

The VDC/MA-1 copolymer is also semicrystalline. For this copolymer, it may be expected that the MA moieties are positioned at crystal chain folds and that the carbonyl functionality is external to the crystal interior.¹⁴ Thermal aging of this resin under a nitrogen atmosphere initiates processes similar to those observed for the VDC/VC-1 resin; the VDC/MA-1 resin shows a slight increase in molecular weight up to ~ 3 h and then a very rapid increase. The rapid increase after ~ 3 h is probably reflective of significant crystallite destruction, whereas the minimal increase before this time is suggestive of more chain flexibility in this crystal structure than in the VDC/VC-1 structure. Thermal degradation of the VDC/MA-1 resin in air is distinctly different from that of its VC counterpart. In air, there is rapid oxidative chain-scission of the crystallite structure, probably at the more exposed MA groups,¹⁵ followed by rapid cross-linking.

Degradation Under Shear

Shear stress should directly affect the thermal processes of chain-scission and cross-linking. These effects can be studied using a torque rheometer, such as a Brabender Plasti-Corder. Inherent in the use of a torque rheometer are the assumptions that the resin sample experiences some average shear rate ($\dot{\gamma}$) and shear stress (τ) and that the rpm values of the rotor blades (S_D , S_S) are directly proportional to $\dot{\gamma}$ and the torque is directly proportional to τ . The validity of these latter two assumptions has been elegantly demonstrated by Goodrich and Porter.¹⁶

The oven-aging studies have shown that VDC copolymers undergo cross-linking in the absence and

presence of oxygen and chain-scission only in the presence of oxygen. These reactions appear to also occur under shear. Therefore, mathematical equations that model these processes are needed if the effect of shear is to be studied. The derivation of a kinetic equation for a cross-linking process under shear for VDC copolymers is given in Appendix A. The derivation of a kinetic equation for chain-scission under shear for VDC copolymers is given in Appendix B. Specifically, the equation for cross-linking is

$$\frac{dx}{dt} = [\tau^n A_x \exp(-E_{Ax}/RT)] \times (X - x)(NEP)^2(1 + PO) \quad (8)$$

where dx/dt is the rate of cross-link formation; τ , the shear stress; n , a constant; A_x , the nonshear component of the preexponential factor; E_{Ax} , the activation energy of cross-linking; R , a gas constant; T , the temperature; (NEP) , the n -ene polyenes (normally dienes¹⁷); X , the maximum level of attainable cross-links; x , the number of cross-links at time t ; $PO = f(O_2)$, and

$$k_x = \tau^n A_x \exp(-E_{Ax}/RT) \quad (9)$$

where k_x is the rate constant of cross-linking.

The kinetic equation for chain-scission is

$$\frac{dc}{dt} = [\tau^m A_s \exp(-E_{As}/RT)](\rho O_2)^q \quad (10)$$

where dc/dt is the rate of chain-scission; τ , the shear stress; m , a constant; A_s , the nonshear component of the preexponential factor; E_{As} , the activation energy of chain-scission; R , a gas constant; T , the temperature; (ρO_2) , the partial pressure of oxygen available to be involved in the chain-scission process; q , a constant, and

$$k_s = \tau^m A_s \exp(-E_{As}/RT) \quad (11)$$

where k_s is the rate constant for chain-scission.

Chain-scission and cross-linking both occur during shear degradation; the net rate of bond formation (db/dt) is

$$\frac{db}{dt} = \frac{dx}{dt} - \frac{dc}{dt} \quad (12)$$

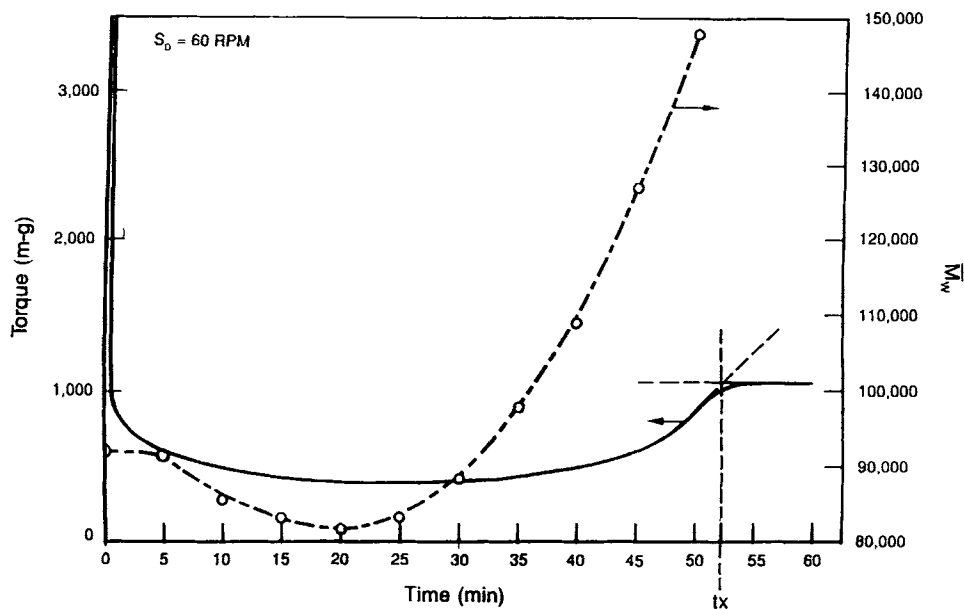


Figure 3 Torque and molecular weight changes for VDC/VC-2 resin degraded under shear in air ($T_{\text{melt}} \approx 172^{\circ}\text{C}$).

The process in air can be represented as

$$\frac{db}{dt} = k_x(X-x)(NEP)^2(1+PO) - k_s(\rho O_2)^q \quad (13)$$

and, in the absence of oxygen,

$$\frac{db}{dt} = k_x(X-x)(NEP)^2 \quad (14)$$

The rate expressions given in eqs. (8)–(14) represent only the shear-related components of chain-scission and cross-linking and do not include the purely thermal components of these processes. Any complete kinetic expression must account for the presence of both processes. As a first approximation, it is assumed that the thermal components of these processes are much smaller in magnitude than the shear-related components and that the above equations represent the major processes that occur under shear. It is also assumed that all volume elements undergo shear at some time.[†]

Chain-scission and cross-linking occur concurrently during the thermal degradation in air under shear for VDC copolymers. There are times, how-

ever, when one type of reaction takes precedence over another. At the onset of thermal degradation, oxidative chain-scission appears to take precedence to cross-linking, whereas in latter times, cross-linking takes precedence (see Fig. 3 and also Table I).

Work by Lisitskii et al.¹⁸ on the mechanochemical degradation of PVC has indicated that oxidative chain-scission of the resin occurs at isolated C,C-double bonds; the level of isolated C,C-double bonds present was monitored by ozonization and was shown to decrease during the early stages of the PVC comminution. Kelen¹⁹ indicated that cyclic peroxides are formed by the thermal oxidation of conjugated polyenes and suggests that these structures are stabilized against chain-scission, by implication indicating that oxidative chain-scission in PVC occurs at isolated C,C-double bonds in preference to conjugated polyene sequences.

In VDC copolymers, the highest concentration of isolated C,C-double bonds appears to occur during the early stages of dehydrochlorination. During these early stages, shear-enhanced oxidative chain-scission should occur; this appears to be what is observed in this study. Shear should accelerate this reaction in three ways: (1) It should increase the rate of contact of molten VDC copolymer with the oxidative atmosphere; (2) it should increase the probability that any particular isolated C,C-double bond in the polymer chain would come in contact with oxygen and it should increase the average life-time of that contact; and (3) it could change the

[†] This may not be true at low shear rates; the definition of "low" depends on the torque rheometer configuration as well as the rate and duration of reaction.

Table I Molecular Weight Data for VDC/VC-1 Resin Degraded Under Shear in Air

S_D (rpm)	T_{Melt} (°C)	t (min)	M_n (M.W.U.)	M_w (M.W.U.)	M_w/M_n	S_D (rpm)	T_{Melt} (°C)	t (min)	M_n (M.W.U.)	M_w (M.W.U.)	M_w/M_n	
40	—	0	28,945	100,978	3.49	60	177	25	36,014	98,850	2.74	
	170	5	27,867	92,671	3.33		177	30	35,452	108,322	3.06	
	172	10	29,899	97,596	3.26		179	35	35,426	128,854	3.64	
	172	15	30,199	91,299	3.02		183	40	36,739	159,597	4.34	
	172	20	28,544	90,356	3.17		186	45	11,481	121,328	10.57	
	172	25	29,255	88,273	3.02		—	0	38,636	97,171	2.52	
	172	30	26,876	84,258	3.14		181	5	37,095	93,228	2.51	
	172	35	28,076	94,763	3.38		181	10	35,116	85,566	2.44	
	171	40	29,415	93,262	3.17		180	15	32,969	82,605	2.51	
	172	45	28,975	104,459	3.61		180	20	32,385	84,830	2.62	
	172	50	25,543	98,951	3.87		180	25	31,893	97,516	3.06	
	173	55	32,064	128,220	4.00		181	30	32,513	119,840	3.69	
	40	—	0	29,871	87,014		2.91	60	183	35	32,222	140,439
178		5	24,396	72,675	2.98	187	40		18,275	124,182	6.80	
180		10	26,764	75,037	2.80	—	0		40,124	96,691	2.41	
181		15	23,795	68,356	2.87	184	5		38,989	90,600	2.32	
181		20	22,543	68,557	3.04	185	10		35,880	83,281	2.32	
181		25	25,158	93,791	3.73	185	15		35,023	85,584	2.44	
181		30	28,882	100,646	3.48	186	20		33,675	93,949	2.79	
181		35	27,899	119,715	4.29	190	25		33,698	115,540	3.43	
—		0	34,921	98,218	2.81	197	30		33,652	148,381	4.41	
60	173	5	36,660	95,061	2.59	80	—	0	36,504	95,562	2.62	
	173	10	34,949	90,744	2.60		173	5	33,449	95,530	2.86	
	172	15	31,879	91,471	2.87		174	10	31,354	90,264	2.88	
	172	20	33,236	83,874	2.52		174	15	33,003	84,866	2.57	
	171	25	30,593	85,846	2.81		173	20	30,118	82,116	2.73	
	171	30	30,400	93,445	3.07		173	25	27,022	82,126	3.04	
	172	35	30,114	93,198	3.09		173	30	26,825	90,819	3.39	
	172	40	30,271	100,981	3.34		175	35	29,987	120,667	4.02	
	173	45	30,621	121,634	3.97		—	0	36,274	96,894	2.62	
	178	50	31,535	151,643	4.81		178	5	28,614	88,388	3.09	
	179	55	27,949	140,191	5.02		180	10	28,192	80,440	2.85	
	60	—	0	48,880	101,079		2.07	181	15	29,204	81,084	2.78
		176	5	39,253	98,470		2.51	181	20	29,304	89,008	3.04
177		10	38,700	95,033	2.46	181	25	27,027	101,619	3.76		
177		15	37,669	91,570	2.43							
177		20	41,538	92,825	2.23							

S_D = rpm of drive blade (drive blade rpm/slave blade rpm = 3/2), T_{Melt} = temperature of resin at time (t), M_n = number-average molecular weight, M_w = weight-average molecular weight, and M.W.U. = molecular weight units (grams/mole).

C,C-double bond moiety, making it more susceptible to oxygen attack. All of these could be manifest by apparent changes in the Arrhenius preexponential factor.

Cross-linking in VDC copolymers appears to occur via a Diels–Alder condensation.²⁰ The Diels–Alder condensation minimally requires the presence of one conjugated diene and a single C,C-double bond. The diene can exist in two forms: *s-cis* and *s-*

trans. The *s-cis* form is required for the Diels–Alder reaction.²¹ According to Wypych,²² the cross-linking is a stereospecific process requiring *cis-transoid* and *trans-cisoid* structures. Applied to PVC and VDC copolymers, this imposes the requirement of high stereoselectivity and for the presence of polyenes larger than dienes.

The Diels–Alder cross-linking requires at least conjugated dienes and possibly trienes and tetraenes,

species that do not occur in the polymer in the early stages of dehydrochlorination. What is observed for VDC copolymers under shear is that cross-linking appears to have an induction period before the process is detectable, possibly the generation of sufficient polyenes to allow the process to noticeably occur. In PVC, cross-linking occurs, to a much lesser extent, via free radical branching.²³ This is believed to be a minor contributor to cross-linking in VDC copolymers.

Shear should accelerate cross-linking in VDC copolymers in at least three ways: (1) It could enhance dehydrochlorination, either by direct shear-stress inducement or by increasing oxygen availability to the polymer; (2) it could orient the polymer chains into the proper *cisoid/transoid* conformations; and (3) it could increase the probability that two polymer chains could interact to allow cross-linking.

It is interesting to consider the mechanism by which shear would enhance the process of dehydrochlorination. Oxygen-accelerated dehydrochlorination is well known for PVC²⁴ and might be expected for VDC copolymers. A weight loss of ~ 2–3% HCl was measured for the VDC copolymers when they were thermally degraded in air (no shear) for 50 min at 172°C. For a VDC/VC copolymer sheared at 60 rpm at ~ 172°C, after 50 min under shear, ~ 2–4% HCl weight loss was estimated. These data indicate that shear stress does not grossly accelerate the rate of dehydrochlorination, but do not rule out the possibility of a slight increase in the rate of dehydrochlorination due to shear.

If shear accelerates both oxidative chain-scission and oxidative and nonoxidative cross-linking, then shear-accelerated oxidative chain-scission should be auto-decelerating and shear-accelerated cross-linking should be auto-accelerating. The chain-scission process should be auto-decelerating because as chain-scission proceeds the molecular weight of the resin decreases, decreasing the shear stresses, further decreasing the rate of reaction. It is even possible that the molecular weight would decrease to such a low value that some minimum shear stress would occur that would be insufficient to accelerate the process; this point of occurrence will be defined as that with limiting-molecular weight (MW_1) and limiting-shear stress (τ_1). Conversely, the cross-linking process should be auto-accelerating; as cross-linking proceeds, the molecular weight of the resin increases, increasing the shear stresses, further accelerating the rate of reaction. As above, a minimum shear stress is probably needed to accelerate the cross-linking process.

Table II Cross-linking Data for Vinylidene Chloride Copolymers Degraded Under Shear in Air

Resin	S_D (rpm)	T_{Melt} (m-g)	Min Torq (min)	t_x (m-g)	X-L Torq
VDC/VC-1	40	172	350	67.00	600
	40	181	290	44.25	690
	60	171	380	58.85	520
	60	172	420	54.00	590
	60	176	350	49.25	560
	60	177	420	41.65	580
	80	181	310	39.60	500
	80	181	320	39.50	620
	60	185	320	31.00	640
	60	184	300	32.00	670
	80	173	440	42.75	520
	80	181	350	33.00	600
VDC/VC-2	60	172	380	58.00	650
	60	172	430	52.50	600
	60	172	380	57.00	600
	60	172	380	55.75	600
	60	176	380	47.75	600
	60	176	280	49.20	570
	60	180	300	42.75	580
	60	181	330	36.75	620
	60	184	250	36.25	550
	60	184	280	32.50	600
VDC/VC-3	60	176	630	37.00	630
	60	176	550	28.25	690
	60	181	570	24.00	760
	60	180	550	24.00	600
	60	183	460	22.75	650
	60	184	500	21.00	600
	60	187	470	19.20	680
	60	187	400	20.00	600
	VDC/MA-1	40	172	360	68.00
40		181	250	41.75	700
60		173	480	53.75	800
60		173	460	53.50	800
60		177	370	45.75	750
60		177	360	45.00	720
60		181	330	38.25	800
60		181	350	36.25	770
60		184	300	31.00	740
60		185	310	30.25	870
80		172	420	44.25	670
80	181	360	31.25	750	

S_D = rpm of drive blade (drive blade rpm/slave blade rpm = 3/2), T_{Melt} = average temperature of resin during the shearing process, before onset of major cross-linking, Min Torq = minimum measured torque during the shearing process, t_x = time for the completion of the cross-linking process, X-L Torq = change in torque due to the cross-linking process, m-g = meter-grams.

Degradation Under Shear in Air

Thermal degradation under shear in air will be discussed first because it corresponds to the most common way to carry out experiments in a torque rheometer. This type of degradation is most complex for VDC copolymers because both chain-scission and cross-linking occur.

Three VDC/VC copolymers and one VDC/MA copolymer were thermally degraded under shear in an air atmosphere in a torque rheometer. Torque rheological and molecular weight data were obtained for these resins under different temperatures and shear rates. In all cases, increasing either shear rate or temperature increased the rates of oxidative chain-scission and cross-linking. The data clearly show that the Brabender cross-linking time (t_x) is decreased both by increasing shear rate (rpm) or by increasing temperature (see Table II).

The easiest process to study is cross-linking, sim-

ply because it is the most apparent process from the torque/time data. As shown in Appendix A,

$$1/t_x \propto k_x \quad (15)$$

where t_x is the cross-linking time, and k_x , the cross-linking rate constant. The derivations also predict [see eq. (A.20)] that at constant shear rate

$$\ln\left(\frac{1}{t_x}\right)_{\dot{\gamma}} = \left(\frac{nE_F - E_{Ax}}{RT}\right) + \text{constant} \quad (16)$$

where n is a constant; E_F , the activation energy of flow at constant $\dot{\gamma}$; and E_{Ax} , the activation energy of cross-linking, or that a plot of $\ln(1/t_x)_{\dot{\gamma}}$ vs. $(1/T)$ should afford a straight line with a slope of $[(nE_F - E_{Ax})/R]$; this is confirmed in Figure 4. The three low molecular weight resins ($M_w = 91,000 \rightarrow 103,000$) appear to cross-link identically, whereas

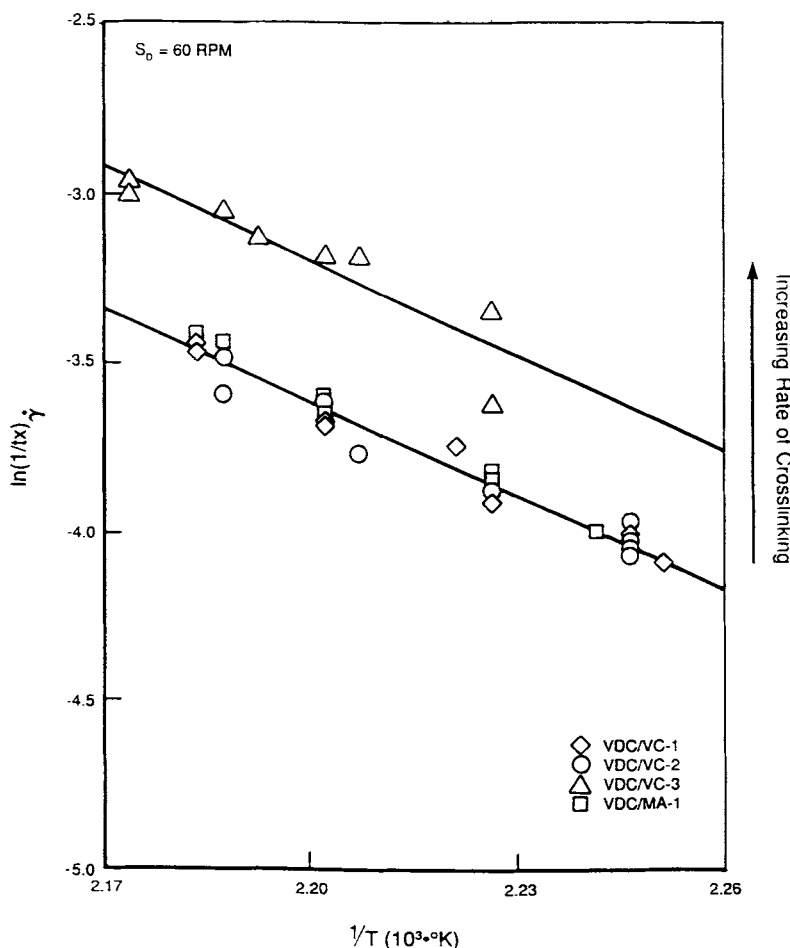


Figure 4 Arrhenius plot for the cross-linking of VDC copolymers under shear in air.

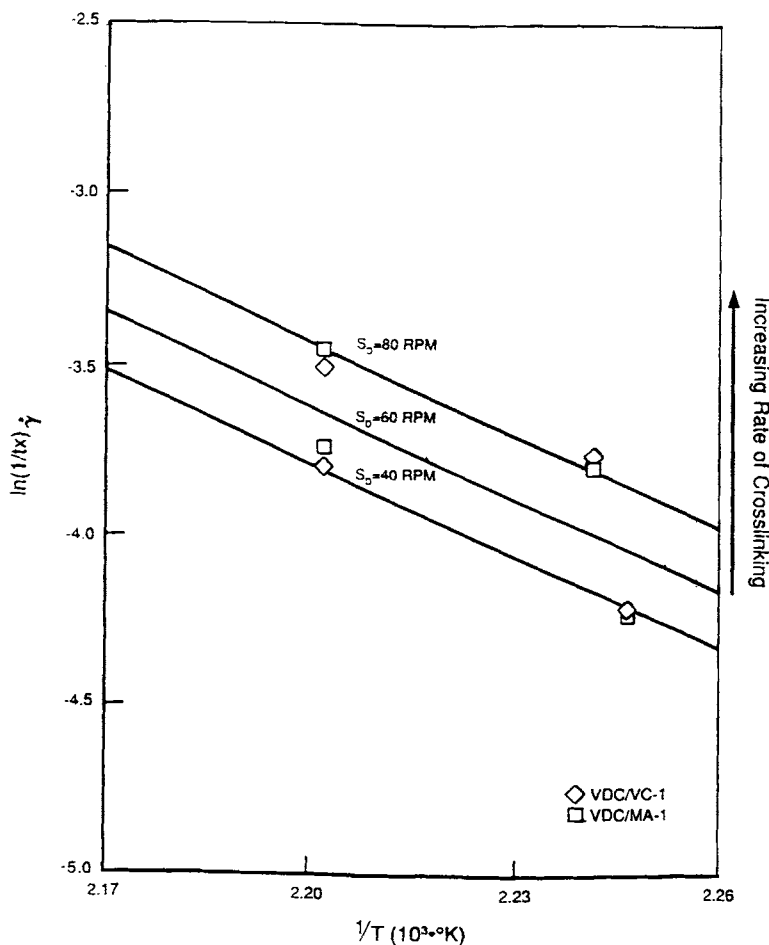


Figure 5 Arrhenius plot for the cross-linking of two VDC copolymers at three different shear rates in an air atmosphere.

the higher molecular weight resin ($M_w \approx 127,000$) cross-links functionally the same as do the three other resins, but at a faster rate. This rate and zero-intercept difference is related to the molecular weights of these resins at the onset of cross-linking; the different molecular weights result in different shear stresses on the resins. The higher the molecular weight, the higher the shear stress and the corresponding rate of cross-linking. The solid lines in Figure 4 are the least-squares straight-line fit of the data. The equations for the two lines are $y = -9,309x + 17.285$ ($R = -0.987$) for the VDC/VC-3 resin and $y = -9,066x + 16.332$ ($R = -0.979$) for the other three VDC copolymers ($R =$ correlation coefficient).

The effect of molecular weight on the cross-linking time can be illustrated by rewriting eq. (16) as

$$\ln\left(\frac{1}{t_x}\right)_T = n \ln \dot{\gamma} + n \ln C_{x,\dot{\gamma}} + \text{constant}' \quad (17)$$

where $C_{x,\dot{\gamma}}$ is a constant at a fixed molecular weight and fixed $\dot{\gamma}$ [see eq. (A.19)].

At a fixed shear rate, differences in molecular weight of the cross-linked resin would yield differences in $C_{x,\dot{\gamma}}$ values, resulting in different intercepts for eq. (16). Equation (17) also predicts that for a particular resin changes in shear rate would shift the intercepts of plots of eq. (16), as is demonstrated in Figure 5 (the 60 rpm data are from Fig. 4). All three slopes are identical and independent of shear rate. The zero-intercepts for these lines, b , are at $S_D = 40$ rpm, $b = +16.18$; at $S_D = 60$ rpm, $b = +16.33$; and at $S_D = 80$ rpm, $b = +16.48$. These data graphically show that shear rate accelerates cross-linking. They also show that, for a particular resin, varying the shear stress over a small range will not affect the slope of the Arrhenius plot.

The intercepts of the Arrhenius plot should also vary, for a fixed resin, with the torque at the onset of cross-linking [see eq. (A.32)], or

$$b = n \ln \text{Torq}_{m,T,\dot{\gamma}} + \text{constant}'' \quad (18)$$

where $b = \ln(1/t_x)_{\dot{\gamma}}$ at $(1/T) = 0$, and $\text{Torq}_{m,T,\dot{\gamma}}$ = the minimum Brabender torque, the torque at the onset of cross-linking at T , $\dot{\gamma} = \text{constant}$.

The cross-linking dependency (n) can be obtained from eq. (18). A large data set is desired to reduce the error in this determination. To obtain a large set of b -values to allow a calculation of n , the molecular weight of a VDC copolymer was increased by quiescently thermally aging it. It then was thermally degraded under a fixed shear rate and the time to cross-link $(t_x)_{\dot{\gamma}}$ and the torque at the onset of cross-linking (Torq_m or min Torq) measured. An Arrhenius plot of these data (Table III) was extrapolated to obtain the zero-intercept data.

The value of n can be determined from the slope of b vs. $\ln \text{Torq}_{m,T,\dot{\gamma}}$, as shown in Figure 6. The solid line in Figure 6 fits the equation $y = +1.289x + 8.560$ ($R = 0.943$); the dashed-line, for the data at $T = 181^\circ\text{C}$, was drawn to be parallel to the $T = 172^\circ\text{C}$ data. From these data, a value of $n \simeq +1.3$ is obtained. The value of n can also be obtained from

$$b = n \ln \text{Torq}_{x,T,\dot{\gamma}} + \text{constant}''' \quad (19)$$

where $\text{Torq}_{x,T,\dot{\gamma}}$ = the Brabender torque at t_x , at T , $\dot{\gamma} = \text{constant}$. A plot of b vs. $\ln \text{Torq}_{x,T,\dot{\gamma}}$ should yield a straight line. From the slope of these data, a value of $n \simeq +1.6$ is obtained.

It is possible to study the cross-linking process by following changes in the molecular weight and molecular weight distribution of the VDC copolymers thermally degraded under shear in an air atmosphere. However, before this can be done, a knowledge of the preceding chain-scission process is necessary. The kinetic derivations for oxidative chain-scission under shear are given in Appendix B. These derivatives show that the rate of chain-scission can be defined by changes in the number-average molecular weight (M_n) or

$$\left(\frac{1}{M_{n_t}} - \frac{1}{M_{n_0}} \right) \cdot \frac{1}{t} = NRCS \quad (20)$$

where M_{n_t} is the number-average molecular weight at time = t ; M_{n_0} , the number-average molecular weight at zero time; and $NRCS$, the number-average rate of chain-scission (the units are moles of polymer chains/g-min); this is the apparent rate constant for chain scission (k_s). The changes in molecular

Table III Torque Data for the Crosslinking of Vinylidene Chloride Copolymers Under Shear in Air

Resin	T_{Melt} (°C)	S_D (rpm)	Min Torq (m-g)	t_x (min)	X-L Torq (m-g)	b
VDC/VC-2	172	60	430	54	550	+16.36
	172	60	490	47	550	+16.50
	172	60	500	40	650	+16.66
	172	60	520	38	600	+16.71
	172	60	580	33	600	+16.85
	172	60	700	24	550	+17.17
	172	60	700	24	400	+17.17
VDC/MA-1	172	60	490	53	700	+16.38
	172	60	510	48	750	+16.48
	172	60	600	39	800	+16.69
	172	60	600	35	800	+16.80
	172	60	700	31	800	+16.92
	172	60	800	24	800	+17.17
	172	60	1100	18	500	+17.46
	172	60	1100	15	500	+17.64
VDC/VC-1	181	60	310, 320	40, 40	500, 620	+16.33
VDC/VC-2	181	60	300, 330	43, 37	580, 620	+16.33
VDC/VC-3	180	60	570, 550	24, 24	760, 600	+17.29
VDC/MA-1	180	60	330, 350	38, 36	800, 770	+16.33

T_{Melt} = average temperature of the resin during the shearing process, before onset of major cross-linking, S_D = rpm of drive blade (drive blade rpm/slave blade rpm = 3/2), Min Torq = minimum measured torque during shearing process, Torq_x = torque at t_x (the cross-linking time), m-g = meter-grams, $b = \ln(1/t_x)$ at $(1/T) = 0$, from Arrhenius plots in Figure 6.

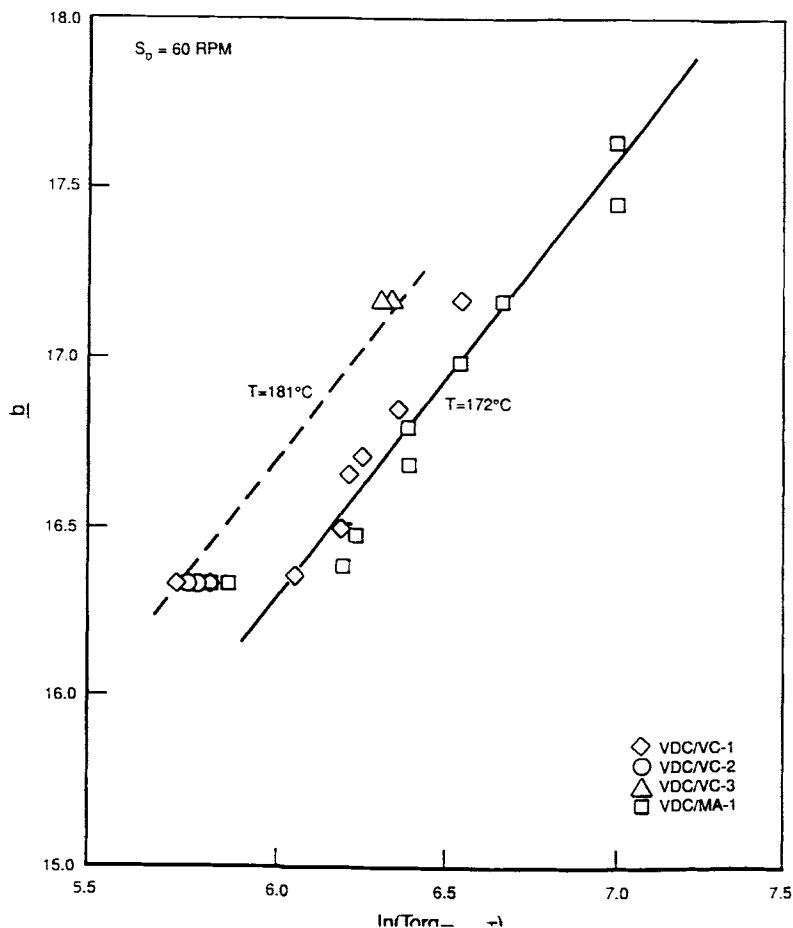


Figure 6 Plot of b vs. $\ln(\text{Torque}_{m, \dot{\gamma}, T})$ for the shear-induced degradation of VDC copolymers in air.

weight for the VDC copolymers thermally degraded under shear in an air atmosphere were obtained and used to determine the $NRCS$ values.

The kinetic derivation for chain-scission shows that at constant shear rate and for a small amount of chain-scission in an air atmosphere that

$$\ln(NRCS)_{\dot{\gamma}} \approx \left(\frac{mE_F - E_{As}}{RT} \right) + \text{constant} \quad (21)$$

where m is a constant; E_F , the activation energy of flow at constant $\dot{\gamma}$; and E_{As} , the activation energy of chain-scission, or that a plot of $\ln(NRCS)_{\dot{\gamma}}$ vs. $(1/T)$ should yield a straight line with a slope of $[(nE_F - E_{As})/R]$. For VDC/VC copolymers, the Arrhenius plot of chain-scission is given in Figure 7 (see Table IV). The equation for the least-squares solid straight line is $y = -11,167x + 9.431$ ($R = -0.772$). The dashed line is drawn to be parallel to the least-squares-fit straight line.

The high molecular weight resin appears to have the same functionality of chain-scission as that of the two low molecular weight resins, but undergoes chain-scission at a greater rate under equivalent conditions. Again, the higher the molecular weight, the greater the shear stress and rate of chain-scission.

The chain-scission data appear to have more scatter than do the cross-linking data shown in Figure 4. Two major factors contribute to the scatter: First, periodically, about 0.2 g of resin sample was removed for molecular weight analyses; this represents $\sim 0.3\%$ of the resin. Samples were removed every 5 min. Under low shear conditions, these samples may not be totally representative of the whole sample. Second, equally important is the derivation of eq. (21). The error in $\ln(NRCS)$ is $\pm mr \ln(Mw_t/Mw_0)$ [see eq. (B.19)–(B.21)]; the error is $\sim \pm mr \cdot \ln(80,000/90,000)$ or $\sim \pm mr(0.12)$. Large values of mr would greatly magnify this error [if mr

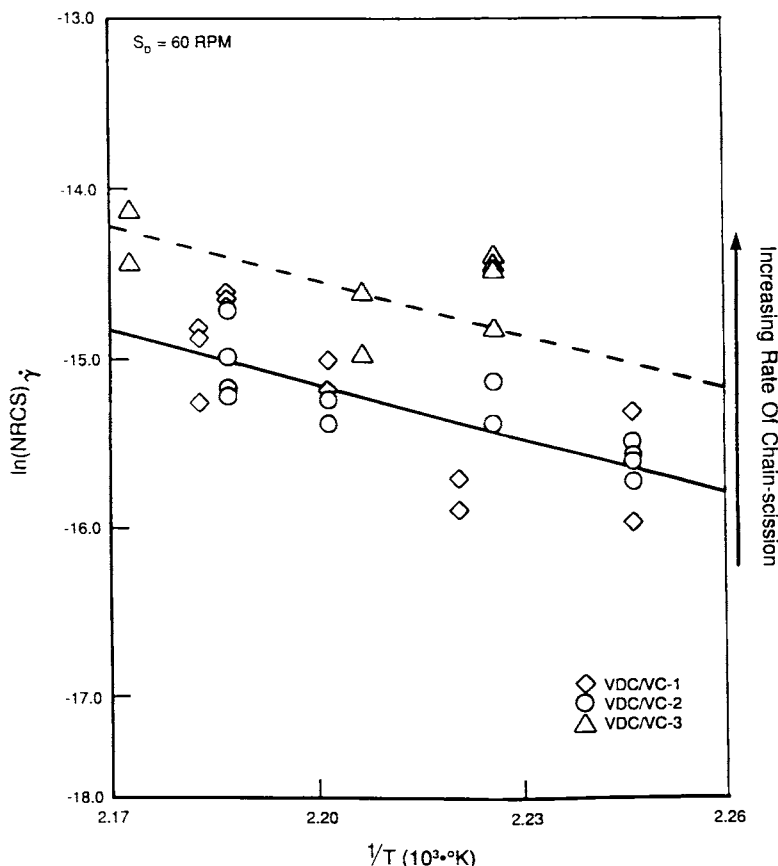


Figure 7 Arrhenius plot for the chain-scission of VDC/VC copolymers under shear in air.

$= 3$, the error in the $\ln(NRCS)$ data will be about ± 0.4 , the error observed in Fig. 7].

Using eq. (B.39), a value of $m \approx +1.1 \pm 0.4$ can be estimated. Likewise, using eq. (B.40), a value of $mr \approx +2.2 \pm 0.8$ can be estimated. A more direct way to calculate m would be to follow the rate of chain-scission under different shear-rate conditions. At low shear rates, inhomogeneities in the sample introduce large errors in $\ln(NRCS)$ values and make this procedure difficult to apply.

As noted previously, oven aging studies have shown that the MA copolymer can undergo oxidative chain-scission at the MA mer-unit. This occurrence could greatly impact the activation energy of chain-scission for the VDC/MA copolymer if either the MA chain-scission was so extensive as to grossly affect the kinetics of the system or the MA scission was the rate-limiting step. The Arrhenius plot for the chain-scission of the VDC/MA copolymer at $S_D = 60$ rpm in an air atmosphere is displayed in Figure 8. The solid line represents the least-squares straight-line fit for the data; the equation for that line is $y = -1545x - 11,220$ ($R = -0.245$).

A comparison of the data in Figures 7 and 8 shows that the Arrhenius slope for the VDC/VC resins ($-11,167$ K) is appreciably different from that of the VDC/MA resin (-1545 K) and that the Arrhenius intercepts ($+9.431$ and -11.220) are, respectively, also different. The activation energies of flow (E_F) for these resins should be almost identical. Therefore, according to eq. (21), the differences in slope can be due to either differences in m -values and/or differences in the activation energy of chain-scission (E_{As}). Either or both differences support different chain-scission mechanisms for the VDC/VC and VDC/MA copolymers, as previously postulated. The difference in mechanisms involves oxidative chain-scission of the MA groups; their exact involvement, however, awaits further elucidation.

It is of interest now to reconsider the auto-decelerating nature of the chain-scission process. Equation (19) does not correct for this auto-deceleration process; hence, the large scatter in the Arrhenius plot data. The auto-deceleration correction is $mr \ln(M_{wt}/M_{w0})$, as discussed previously. The point of maximum auto-deceleration of chain-scis-

Table IV Rate Constants for Chain-Scission of Vinylidene Chloride Copolymers Degraded Under Shear in Air

Resin	S_D (rpm)	T_{Melt} (°C)	k_s (mol/g min)	PD	k'_s (mol/g min)	$k'_s \cdot PD$ (mol/g min)	
VDC/VC-1	40	172	3.62×10^{-8}	3.20	5.57×10^{-8}	1.78×10^{-7}	
	40	181	4.55×10^{-7}	2.89	1.41×10^{-7}	4.08×10^{-7}	
	60	172	1.17×10^{-7}	2.70	8.32×10^{-8}	2.25×10^{-7}	
	60	177	1.26×10^{-7}	2.37	6.43×10^{-8}	1.52×10^{-7}	
	60	181	2.58×10^{-7}	2.52	1.20×10^{-7}	3.04×10^{-7}	
	60	185	2.38×10^{-7}	2.37	1.56×10^{-7}	3.70×10^{-7}	
	60	185	3.48×10^{-7}	2.07	1.68×10^{-7}	3.48×10^{-7}	
	80	173	3.23×10^{-7}	2.62	9.49×10^{-8}	2.49×10^{-7}	
VDC/VC-2	60	172	1.48×10^{-7}	2.60	7.18×10^{-8}	1.87×10^{-7}	
	60	172	1.68×10^{-7}	2.11	8.17×10^{-8}	1.72×10^{-7}	
	60	176	2.12×10^{-7}	2.54	1.06×10^{-7}	2.69×10^{-7}	
	60	181	2.40×10^{-7}	2.62	8.01×10^{-8}	2.10×10^{-7}	
	60	184	4.10×10^{-7}	2.53	1.27×10^{-7}	3.21×10^{-7}	
	60	184	2.49×10^{-7}	2.10	1.50×10^{-7}	3.16×10^{-7}	
	VDC/VC-3	60	176	5.57×10^{-7}	2.13	2.50×10^{-7}	5.32×10^{-7}
		60	176	3.67×10^{-7}	2.07	2.50×10^{-7}	5.17×10^{-7}
60		180	3.11×10^{-7}	2.54	1.76×10^{-7}	4.47×10^{-7}	
60		184	4.40×10^{-7}	2.48	1.67×10^{-7}	4.14×10^{-7}	
60		184	4.11×10^{-7}	2.13	2.10×10^{-7}	4.47×10^{-7}	
60		187	5.33×10^{-7}	2.48	2.93×10^{-7}	7.27×10^{-7}	
VDC/MA-1	40	172	1.32×10^{-7}	2.52	7.95×10^{-8}	2.00×10^{-7}	
	40	180	3.55×10^{-7}	2.40	1.73×10^{-7}	4.15×10^{-7}	
	60	172	4.86×10^{-7}	2.32	1.92×10^{-7}	4.45×10^{-7}	
	60	177	5.89×10^{-7}	2.31	2.10×10^{-7}	4.85×10^{-7}	
	60	181	4.08×10^{-7}	2.23	1.60×10^{-7}	3.57×10^{-7}	
	60	185	5.60×10^{-7}	2.16	2.35×10^{-7}	5.07×10^{-7}	
	60	185	5.81×10^{-7}	1.88	2.80×10^{-7}	5.27×10^{-7}	
	80	173	8.38×10^{-7}	2.75	2.01×10^{-7}	5.53×10^{-7}	
	80	181	8.66×10^{-7}	2.50	2.27×10^{-7}	5.68×10^{-7}	

S_D = rpm of drive blade (drive blade rpm/slave blade rpm = 3/2), T_{Melt} = average temperature of the resin during the chain-scission process, k_s = rate constant determined from M_n data, $PD = M_w/M_n$, k'_s = rate constant determined from M_w data, and $k_s = k'_s \cdot PD$.

sion is the point of minimum Brabender torque (Torq_m). If auto-deceleration is the sole factor for Torq_m , then a T_1 or MW_1 should be observed. The data show that the three low molecular weight resins have $M_w \approx 83,000$ at Torq_m , whereas the high molecular weight resin has $M_w \approx 99,000$ at Torq_m . The absence of a limiting molecular weight value indicates that auto-deceleration is not the sole contributor to Torq_m and that in this region both chain-scission and cross-linking contribute to Torq_m .

The molecular weights of the resins decrease from the onset of shear-degradation until the time of Torq_m , while maintaining a constant polydispersity (PD). It can be shown that

$$\ln \text{Torq}_{\dot{\gamma}, T} = \ln C_1 - \ln C_2 + r \ln M_w \quad (22)$$

where $\text{Torq}_{\dot{\gamma}, T}$ is the Brabender torque at constant $\dot{\gamma}$ and T ; C_1 and C_2 , constants; r , a constant, at constant T and $\dot{\gamma}$; and M_w , is weight-average molecular weight.

The value of r , the torque-dependency on molecular weight, can be determined from a plot of $\ln \text{Torq}_{\dot{\gamma}, T}$ vs. $\ln M_w$. Molecular weight data and Torq data at constant T and $\dot{\gamma}$, prior to Torq_m , were obtained and plotted according to eq. (22). These data are shown in Figure 9. The least-squares straight line for the data in Figure 9 yields the equation y

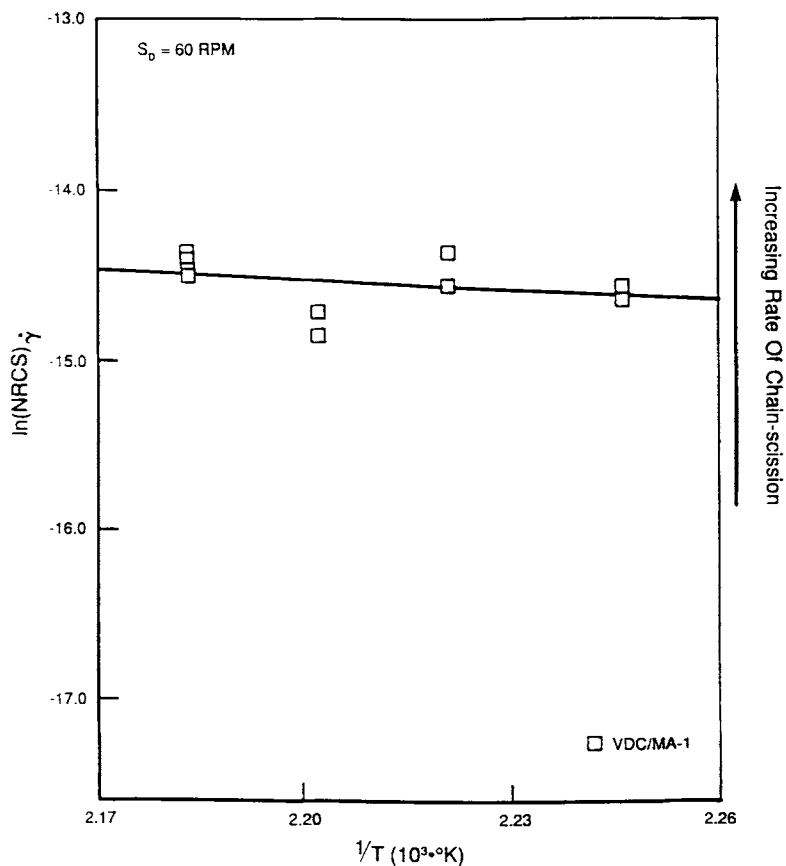


Figure 8 Arrhenius plot for the chain-scission of VDC/MA-1 resin under shear in air.

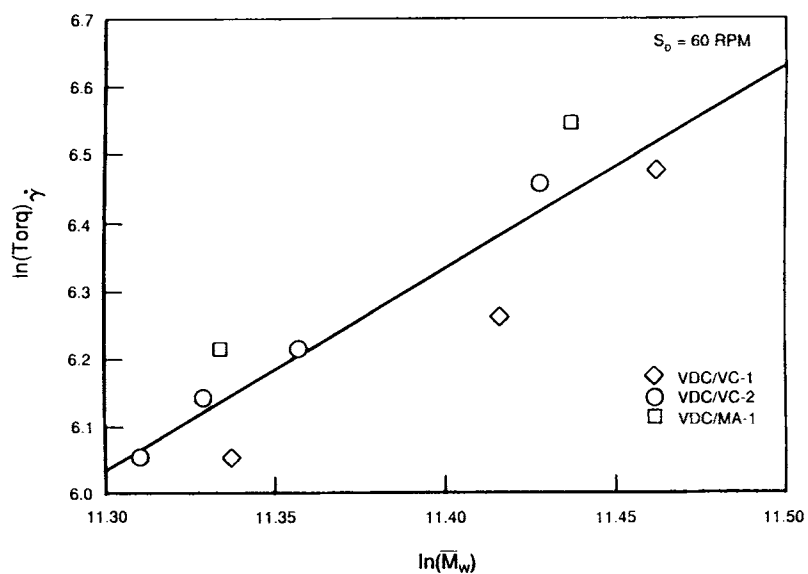


Figure 9 Torque dependency on molecular weight for three VDC copolymers ($T_{\text{melt}} \approx 172^\circ\text{C}$).

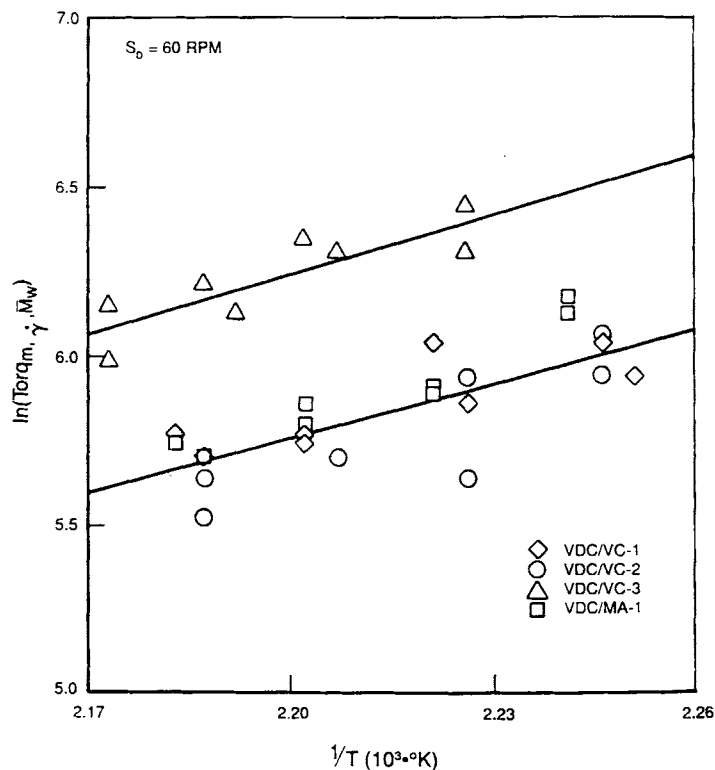


Figure 10 Arrhenius plot of torque data for VDC copolymers in air.

$= +2.99x - 27.800$ ($R = 0.916$), or $r \approx +3.0$ for these resins.

The activation energy of flow (E_F) for these resins can be obtained utilizing the relationship

$$\ln \text{Torq}_{m, M_w, \dot{\gamma}} = \frac{E_F}{RT} + \ln C_3 \quad (23)$$

where C_3 is a constant at constant M_w and $\dot{\gamma}$.

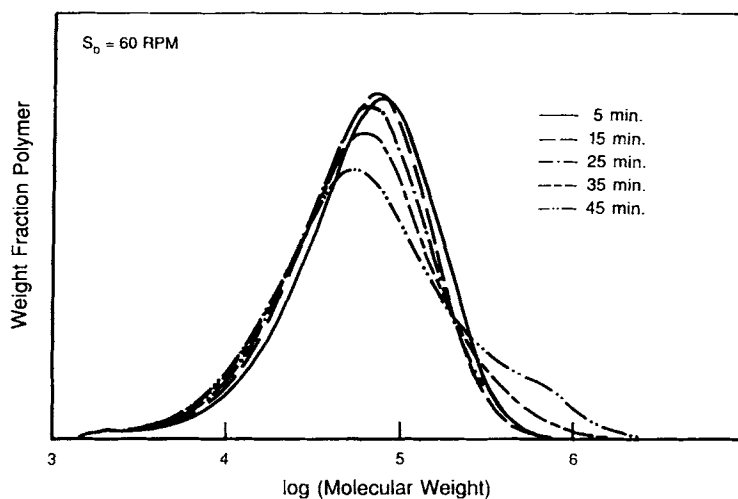


Figure 11 Composite molecular weight distribution curves for VDC/VC-2 resin degraded under shear in air ($T_{\text{melt}} \approx 177^\circ\text{C}$).

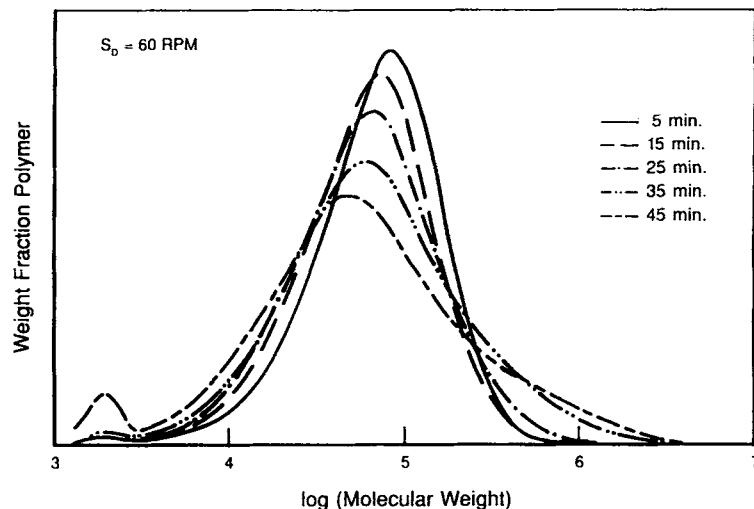


Figure 12 Composite molecular weight distribution curves for VDC/MA-1 resin degraded under shear in air ($T_{melt} \approx 176^\circ\text{C}$).

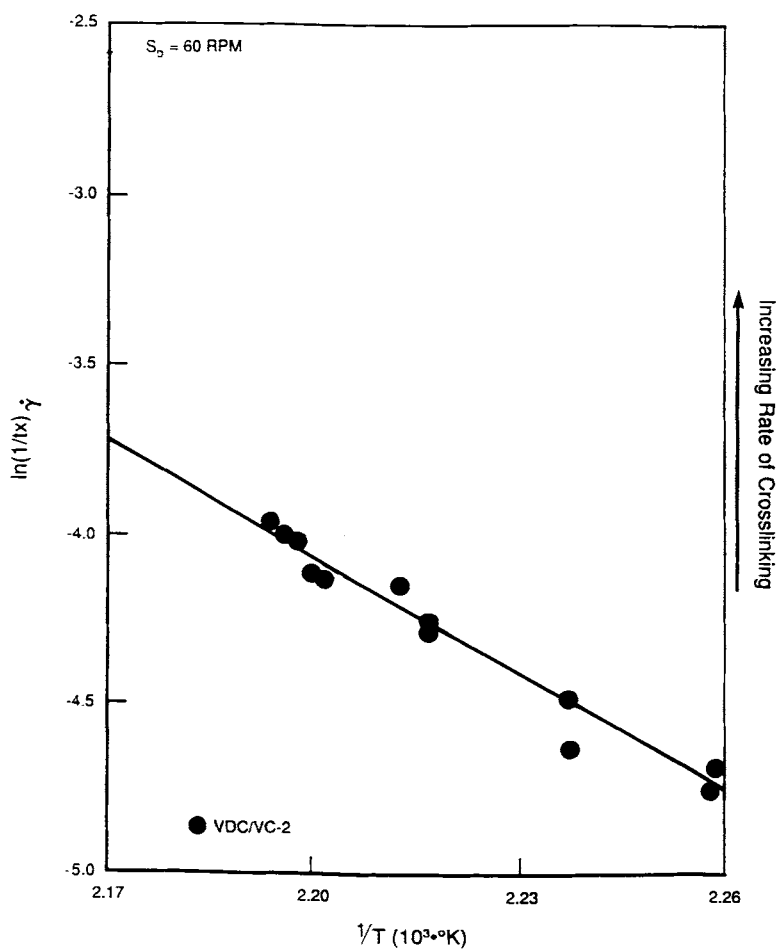


Figure 13 Arrhenius plot for the crosslinking of VDC/VC-2 resin under shear in a nitrogen atmosphere.

Table V Cross-linking Data for Vinylidene Chloride Copolymers Degraded Under Shear in Nitrogen

Resin	S_D (rpm)	T_{Melt} (°C)	Min Torq (m-g)	t_x (min)	X-L Torq (m-g)
VDC/VC-1	60	170	550	108.5	650
	60	169	425	123	500
	60	170	475	116	625
	60	178	400	72.5	700
	60	179	450	63	750
	60	178	420	70.5	680
	60	181	300	62	650
	60	183	425	52.5	800
	60	182	400	54.5	800
	60	182	350	61	675
	60	182	425	55.5	725
	VDC/VC-3	60	170	750	71.5
60		169	700	79.0	325
60		174	750	56.0	500
60		175	500	56.8	400
60		183	425	38.5	525
60		184	525	35.5	625
VDC/MA-1	60	174	450	78.25	875
	60	174	475	77.75	750
	60	177	350	63.25	850
	60	179	450	59.75	975
	60	182	350	51.75	975
	60	182	400	49.0	975

S_D = rpm of drive blade (drive blade rpm/slave blade rpm = 3/2), T_{Melt} = average temperature of resin during the shearing process, before onset of major cross-linking, Min Torq = minimum measured torque during shearing process, t_x = time for the completion of the cross-linking process, X-L Torq = change in torque due to the cross-linking process, and m-g = meter-grams.

Applying eq. (23) to 60 rpm data yields a plot, shown in Figure 10, with least-squares straight-line equations of $y = +5363.2x - 6.0359$ ($R = 0.78$) for the low molecular weight resins and $y = +5885.5x - 6.7007$ ($R = 0.85$) for the high molecular weight resins. From these equations, $E_F = +10.7$ kcal/mol and $+11.7$ kcal/mol, respectively.

From the straight-line fit of the data in Figure 9, $r \simeq +3.0$, with $m \simeq +1.1 \pm 0.4$ (calculated previously), $mr \simeq +3.3 \pm 1.2$ (in good agreement with $mr \simeq +2.2 \pm 0.8$ previously calculated). From the straight-line equations of Figures 4 and 10, it is possible to apply eq. (A.39) and calculate at $T = 187.68^\circ\text{C}$, $n \simeq 0.9 \pm 0.2$, and at $T = 169.33^\circ\text{C}$, $n \simeq 0.8 \pm 0.2$ (at $S_D = 60$ rpm).

The changes in molecular weight distributions for

the VDC/VC-2 and the VDC/MA-1 resins when they are thermally degraded in air ($S_D = 60$ rpm) are shown in Figures 11 and 12, respectively. The impact of both chain-scission and cross-linking is readily apparent in these figures.

Degradation Under Shear in Nitrogen

Thermal degradation under shear in a nitrogen (nonoxidative) environment is a much simpler process than that in an air environment. The cross-linking process under nitrogen should be similar to that in air and should yield the same Arrhenius slope, according to eq. (16), if oxygen does not participate in the rate-limiting step. The Arrhenius plot for the cross-linking process (Table V) under nitrogen for the VDC/VC-2 resin is given in Figure 13. The straight-line least-squares equation for the plot of data obtained for decomposition under nitrogen is $y = -11,552.6x + 21,359$ ($R = -0.984$). The slope can be considered, within experimental error, to be equivalent to that obtained for shear degradation in air.

According to the previous discussion, oxidative chain-scission should not occur during thermal degradation under shear in a nitrogen atmosphere and could be verified by monitoring Torq_m values. The Torq_m values are higher for shear degradation in nitrogen (less chain-scission) than in air. Plotting these Torq_m values vs. $1/T$, according to eq. (20), yields $E_F = +8.2$ kcal/mol for the VDC/VC-2 resin and $E_F = +11.7$ kcal/mol for the VDC/VC-3 resin, in good agreement with the previous E_F values determined for the resins rheometrically examined in an air atmosphere (see Table VI). For the nitrogen atmosphere cross-linking data, values of $n = +1.4$ to $+1.6$ are calculated (at $S_D = 60$ rpm).

MODEL ASSUMPTIONS AND LIMITATIONS

The model to assess the effect of shear stress on the thermal chain-scission and cross-linking of VDC copolymers appears to fit the torque rheological data quite well. The data show that shear stress must be accounted for in studying the kinetics of degradation for these systems. Data fit to the model indicate that shear stress accelerates the chain-scission and cross-linking processes. Finally, the torque rheometer is a useful tool for studying the thermal degradation of VDC copolymers.

However, this first approximation model has several limitations that may need to be addressed in

Table VI Kinetic Constants for the Degradation of Vinylidene Chloride Copolymers Under Shear

Constant	Calculated Value	Conditions	Method of Calculation
$(nE_F - E_{Ax})/R$	-9,066 K	Air, low M_w resins	Eq. (16)
	-9,309 K	Air, high M_w resins	Eq. (16)
	-11,553 K	N ₂ , VDC/VC-2	Eq. (16)
	-11,068 K	N ₂ , VDC/MA-1	Eq. (16)
	-9,826 K	N ₂ , VDC/VC-3	Eq. (16)
n	+1.29 ± 0.39	Air, low M_w resins	Eq. (18) at $T = 172^\circ\text{C}$
	+1.63 ± 0.39	Air, low M_w resins	Eq. (19) at $T = 172^\circ\text{C}$
	+0.9 ± 0.2	Air, all resins	Eq. (A.39) at $T = 187.68^\circ\text{C}$
	+0.8 ± 0.2	Air, all resins	Eq. (A.39) at $T = 169.33^\circ\text{C}$
	+1.6 ± 0.2	N ₂ , VDC/VC resins	Eq. (A.39) at $T = 187.68^\circ\text{C}$
	+1.4 ± 0.2	N ₂ , VDC/VC resins	Eq. (A.39) at $T = 169.33^\circ\text{C}$
$(mE_F - E_{As})/R$	-11,167 K	Air, VDC/VC resins	Eq. (21)
	-1,545 K	Air, VDC/MA resin	Eq. (21)
m	+1.1 ± 0.4	Air, all resins	Eq. (B.39) at $T = 176^\circ\text{C}$
mr	+2.2 ± 0.8	Air, all resins	Eq. (B.40) at $T = 176^\circ\text{C}$
r	+2.0 ± 0.8	Air, all resins	Eqs. (B.39) and (B.40) at $T = 176^\circ\text{C}$
	+2.99	Air, low M_w resins	Eq. (B.41) at $T = 172^\circ\text{C}$
E_F	+10.7 kcal/mol	Air, low M_w resins	Eq. (23)
	+11.7 kcal/mol	Air, high M_w resin	Eq. (23)
	+8.2 kcal/mol	N ₂ , low M_w resin	Eq. (23)
	+11.7 kcal/mol	N ₂ , high M_w resin	Eq. (23)
E_{Ax}	+32 ± 5 kcal/mol	Air, all resins	Table data
	+36 ± 5 kcal/mol	N ₂ , all resins	Table data
E_{As}	+35 ± 5 kcal/mol	Air, VDC/VC resins	Table data
	+16 ± 5 kcal/mol	Air, VDC/MA resin	Table data

All values measured at $S_D = 60$ rpm (where $S_D = \text{rpm}$ of drive rotor blade; rpm drive rotor blade/ rpm of slave rotor blade = 3/2). n = exponent of τ -effect on cross-linking, E_F = activation energy of flow, E_{Ax} = activation energy of cross-linking, m = exponent of τ -effect on chain-scission, E_{As} = activation energy of chain-scission, and x = exponent of molecular weight effect on viscosity.

more detailed studies. The model assumes that the shear stress functionalities (n and m) are constant and independent of τ . This is probably true at the low shear rates (i.e., low shear stresses) studied with the torque rheometer but may not be true at higher shear stresses. It may be that $n, m = f(\tau)$. The model does not address very low shear stress environments (where $\tau^{n,m} \rightarrow 0$), where the non-shear-stress components of the kinetics become dominant. The model assumes that E_F is independent of shear rates (for small shear rate regions, this assumption is valid). Finally, the model assumes that shear stress affects all components of the degradation process equivalently regardless of the extent of degradation. Further work will more precisely fix the importance of all variables for the thermal degradation of VDC copolymers.

APPENDIX A: DERIVATION OF A KINETIC EQUATION FOR A CROSS-LINKING PROCESS UNDER SHEAR FOR VINYLIDENE CHLORIDE COPOLYMERS

The kinetic expressions derived are meant to be approximations of actual phenomena and to demonstrate functional dependency of the process on shear.

Let x = number of cross-links in the polymer system, t = time, X = maximum number of attainable cross-links, and NEP = number of n -ene polyenes per polymer chain.

In the absence of oxygen,

$$\frac{dx}{dt} = k'_x(X - x)(NEP)^2, \quad (\text{A.1})$$

where $\frac{dx}{dt}$ is the rate of cross-link formation, k_x is the rate

constant, $(X - x)$ indicates that the rate of cross-link formation is inhibited by cross-links, and $(NEP)^2$ represents the bimolecular nature of the cross-linking process.¹⁷

In the presence of air,

$$\begin{aligned} \frac{dx}{dt} = & \text{the rate of crosslinking in the absence of oxygen} \\ & + \text{the rate of crosslinking in the presence} \\ & \text{of oxygen} \quad (\text{A.2}) \end{aligned}$$

or

$$\begin{aligned} \frac{dx}{dt} = & k'_x (X - x) (NEP)^2 \\ & + k'_x (X - x) (NEP)^2 (\rho O_2)^p \quad (\text{A.3}) \end{aligned}$$

where (ρO_2) is the partial pressure of oxygen available to be involved in the process and $(\rho O_2)^p$ represents the effect of oxygen on the process; it is raised to the p -power because its effect is unknown ($p = \text{constant}$).

For simplicity, let

$$(\rho O_2)^p \equiv PO \quad (\text{A.4})$$

Substituting eq. (A.4) into eq. (A.3) and rearranging yields

$$\frac{dx}{dt} = k_x (X - x) (NEP)^2 (1 + PO) \quad (\text{A.5})$$

(NEP) varies with t with a functionality that is not exactly known but can be approximated; to solve eq. (A.5), it is necessary to consider the system at $t = t_x$, where t_x is the Brabender cross-linking time, the time at which the change in cross-linking torque is constant and has plateaued. This indicates that a fixed number of cross-links have been established (this is supported by the data in Table II). At $t = t_x$, $(NEP) = \text{constant} = (NEP)_x$.

In a shearing environment that is open to the atmosphere, the amount of available O_2 that can react with the resin is effectively infinite relative to the polymer mass and, therefore, ρO_2 is constant.

Rearranging eq. (A.5), separating variables, isolating constants, integration would yield

$$\int \frac{dx}{(X - x)} = k_x (NEP)_x^2 (1 + PO) \int dt \quad (\text{A.6})$$

Evaluating eq. (A.6) from the limits at $t = 0$, $x = 0$, and at $t = t_x$, $x = x$ yields

$$-\ln(X - x) \Big|_{x=0}^{x=x} = k_x (NEP)_x^2 (1 + PO) t \Big|_{t=0}^{t=t_x} \quad (\text{A.7})$$

or

$$\ln\left(\frac{x}{X - x}\right) = k_x (NEP)_x^2 (1 + PO) t_x \quad (\text{A.8})$$

Let

$$\ln\left(\frac{X}{X - x}\right) = \kappa \quad (\text{A.9})$$

Rearranging,

$$\frac{1}{t_x} = k_x (NEP)_x^2 (1 + PO) \kappa^{-1} \quad (\text{A.10})$$

This equation is useful but does not allow the effect of shear to be determined. To do that, let

$$k_x = A'_x \exp(-E_{Ax}/RT) \quad (\text{A.11})$$

where A'_x is the Arrhenius preexponential factor; E_{Ax} , the activation energy of cross-linking; R , a gas constant; and T , the temperature, and let

$$A'_x = A_x \tau^n \quad (\text{A.12})$$

where τ is the shear stress; n , a constant; and A_x , the non shear component of the preexponential factor, and $A_x \tau^n$ indicates that the probability of reaction is affected by shear.

Substituting eqs. (A.11) and (A.12) into eq. (A.10) and taking the ln of the expression yields an equation that is easily studied with rheometric data, or

$$\begin{aligned} \ln\left(\frac{1}{t_x}\right) = & n \ln \tau_x + \ln A_x - \frac{E_{Ax}}{RT} + 2 \ln(NEP)_x \\ & + \ln(1 + PO) - \ln \kappa \quad (\text{A.13}) \end{aligned}$$

where $\tau = \tau_x$ at $t = t_x$. Recall that

$$\tau = \eta \dot{\gamma} \quad (\text{A.14})$$

where η is the polymer melt viscosity, $\dot{\gamma}$ is the shear rate, and

$$\eta = C_{\dot{\gamma}} \exp(E_F/RT) \text{ at a fixed molecular weight of resin} \quad (\text{A.15})$$

where $C_{\dot{\gamma}}$ is a constant at constant $\dot{\gamma}$ and E_F is the activation energy of flow.

Substituting eqs. (A.14) and (A.15) into Eq. (A.13) yields

$$\ln\left(\frac{1}{t_x}\right) = n \ln \dot{\gamma}_x + n \ln C_{x,\dot{\gamma}} + \frac{nE_F}{RT} + \ln A_x - \frac{E_{Ax}}{RT} + 2 \ln(NEP)_x + \ln(1 + PO) - \ln \kappa \quad (\text{A.16})$$

Let $\dot{\gamma}_x = \dot{\gamma} = \text{constant}$ during the cross-linking process. Then,

$$\ln\left(\frac{1}{t_x}\right) = \left(\frac{nE_F - E_{Ax}}{RT}\right) + n \ln \dot{\gamma} + n \ln C_{x,\dot{\gamma}} + \ln A_x + 2 \ln(NEP)_x + \ln(1 + PO) - \ln \kappa \quad (\text{A.17})$$

$$\text{Let } B = \ln A_x + 2 \ln(NEP)_x + \ln(1 + PO) - \ln \kappa \quad (\text{A.18})$$

Then,

$$\ln\left(\frac{1}{t_x}\right) = \left(\frac{nE_F - E_{Ax}}{RT}\right) + n \ln \dot{\gamma} + n \ln C_{x,\dot{\gamma}} + B \quad (\text{A.19})$$

Equation (A.19) allows an assessment of the activation energy functionality at $\dot{\gamma} = \text{constant}$, $C_{x,\dot{\gamma}} = \text{constant}$, and

$$\frac{\Delta \ln(1/t_x)}{\Delta(1/T)} = \frac{nE_F - E_{Ax}}{R} \quad (\text{A.20})$$

and at $1/T = 0$,

$$b = n \ln \dot{\gamma} + n \ln C_{x,\dot{\gamma}} + B \quad (\text{A.21})$$

where $b = y$ -intercept at $1/T = 0$.

Recall from Goodrich and Porter¹⁶ that for a Brabender Plasti-Corder

$$\eta = \frac{C_1 \text{Torq}}{\dot{\gamma}} \quad (\text{A.22})$$

where C_1 is a constant, dependent on bowl and blades, and Torq is the Brabender torque. Recall, also, eq. (A.15) at $T = \text{constant}$ and $\dot{\gamma} = \text{constant}$:

$$\eta_{\dot{\gamma},T} = C_2 C_{\dot{\gamma}} \quad (\text{A.23})$$

Combining eqs. (A.22) and (A.23) yields

$$C_{\dot{\gamma}} = \frac{C_1 \text{Torq}_{T,\dot{\gamma}}}{C_2 \dot{\gamma}} \quad (\text{A.24})$$

and substituting into eq. (A.21) yields

$$b = n \ln \dot{\gamma} + n \ln C_1 + n \ln \text{Torq}_{x,T,\dot{\gamma}} - n \ln C_2 - n \ln \dot{\gamma} + B \quad (\text{A.25})$$

or

$$b = n \ln \text{Torq}_{x,T,\dot{\gamma}} + n \ln C_1 - n \ln C_2 + B \quad (\text{A.26})$$

or

$$b = n \ln \text{Torq}_{x,T,\dot{\gamma}} + \text{constant} \quad (\text{A.27})$$

and

$$\frac{\Delta b}{\Delta \ln \text{Torq}_{x,T,\dot{\gamma}}} = n \quad (\text{A.28})$$

Equation (A.28) allows a determination of n . Rewriting eq. (A.27) gives

$$b - n \ln \text{Torq}_{x,T,\dot{\gamma}} = \text{constant (independent of } \dot{\gamma}) \quad (\text{A.29})$$

Let

$$\text{Torq}_{x,T,\dot{\gamma}} = C_3 \text{Torq}_{m,T,\dot{\gamma}} \quad (\text{A.30})$$

where $\text{Torq}_{m,T,\dot{\gamma}}$ is the minimum Brabender torque, the torque at the onset of cross-linking at T ; γ , a constant; and C_3 , constant.

Substituting equation (A.30) into eq. (A.26) yields

$$b = n \ln \text{Torq}_{m,T,\dot{\gamma}} + n \ln C_3 + n \ln C_1 - n \ln C_2 + B \quad (\text{A.31})$$

or

$$b = n \ln \text{Torq}_{m,T,\dot{\gamma}} + \text{constant}' \quad (\text{A.32})$$

and

$$\frac{\Delta b}{\Delta \ln \text{Torq}_{m,T,\dot{\gamma}}} = n \quad (\text{A.33})$$

Equation (A.33) allows another determination of n . Also,

$$b - n \ln \text{Torq}_{m,T,\dot{\gamma}} = \text{constant}' \text{ (independent of } \dot{\gamma}) \quad (\text{A.34})$$

The value of n can be determined by another procedure: Recall that

$$\ln\left(\frac{1}{t_x}\right) = n \ln \tau_x + \ln A_x - \frac{E_{Ax}}{RT} + 2 \ln(NEP)_x + \ln(1 + PO) - \ln \kappa \quad (\text{A.13})$$

and, from Goodrich and Porter,¹⁶ that for a Brabender Plasti-Corder

$$\tau = C_4 \text{Torq} \quad (\text{A.14})$$

where C_4 is a constant, dependent on bowl and blades. Then, at $T = \text{constant}$, for resin A,

$$\ln\left(\frac{1}{t_x}\right)_{T,A} = n \ln \text{Torq}_{x,T,A} + n \ln C_4 + \ln A_x - \frac{E_{Ax}}{RT} + 2 \ln(\text{NEP})_x + \ln(1 + PO) - \ln \kappa \quad (\text{A.35})$$

and, at $T = \text{constant}$, for resin B,

$$\ln\left(\frac{1}{t_x}\right)_{T,B} = n \ln \text{Torq}_{x,T,B} + n \ln C_4 + \ln A_x - \frac{E_{Ax}}{RT} + 2 \ln(\text{NEP})_x + \ln(1 + PO) - \ln \kappa \quad (\text{A.36})$$

Then, subtracting eq. (A.36) from (A.35) yields

$$\ln\left(\frac{1}{t_x}\right)_{T,A} - \ln\left(\frac{1}{t_x}\right)_{T,B} = n \ln \text{Torq}_{x,T,A} - n \ln \text{Torq}_{x,T,B} \quad (\text{A.37})$$

Substituting eq. (A.30) into eq. (A.37) yields

$$\ln\left(\frac{1}{t_x}\right)_{T,A,\dot{\gamma}} - \ln\left(\frac{1}{t_x}\right)_{T,B,\dot{\gamma}} = n \ln \text{Torq}_{m,T,A,\dot{\gamma}} - n \ln \text{Torq}_{m,T,B,\dot{\gamma}} \quad (\text{A.38})$$

or

$$\ln\left(\frac{1}{t_x}\right)_{T,A,\dot{\gamma}} - \ln\left(\frac{1}{t_x}\right)_{T,B,\dot{\gamma}} \div [\ln \text{Torq}_{m,T,A,\dot{\gamma}} - \ln \text{Torq}_{m,T,B,\dot{\gamma}}] = n \quad (\text{A.39})$$

The activation energy of flow [E_F] can be independently obtained from torque/molecular weight data.

Recall, also, at $\dot{\gamma} = \text{constant}$, from eq. (A.22)

$$\text{Torq}_{m,\dot{\gamma}} = C_5 \eta \quad (\text{A.40})$$

where C_5 is a constant at constant molecular weight (M_w) and $\dot{\gamma}$ and

$$\eta_{M_w} = C_6 \exp(E_F/RT) \quad (\text{A.41})$$

where C_6 is a constant at constant molecular weight and $\dot{\gamma}$. Then,

$$\text{Torq}_{m,\dot{\gamma},M_w} = C_7 \exp(E_F/RT) \quad (\text{A.42})$$

where C_7 is a constant at constant molecular weight and $\dot{\gamma}$ and

$$\ln \text{Torq}_{m,\dot{\gamma},M_w} = \ln C_7 + \frac{E_F}{RT} \quad (\text{A.43})$$

APPENDIX B: DERIVATION OF A KINETIC EQUATION FOR CHAIN-SCISSION UNDER SHEAR FOR VINYLIDENE CHLORIDE COPOLYMERS

Let $c =$ number of polymer chains. In the presence of oxygen,

$$\frac{dc}{dt} = k_s (\rho O_2)^q \quad (\text{B.1})$$

where $(dc)/(dt)$ is the rate of chain-scission, k_s is the rate constant, (ρO_2) is the partial pressure of oxygen available to be involved in the chain-scission process; $(\rho O_2)^q$ represents the effect of oxygen on the process—it is raised to the q -power because its effect is unknown ($q = \text{constant}$); and $k_s (\rho O_2)^q$ indicates that chain-scission only occurs in the presence of oxygen.

In a shearing environment that is open to the atmosphere, the amount of available O_2 that can react with the resin is effectively infinite relative to the polymer mass; therefore, ρO_2 is constant.

Integrating eq. (B.1) would yield

$$dc = k_s (\rho O_2)^q dt \quad (\text{B.2})$$

Evaluating eq. (B.2) from the limits at $t = 0$, $c = c_0$, at $t = t$, $c = c_t$ yields

$$c \Big|_{c=c_0}^{c=c_t} = k_s (\rho O_2)^q t \Big|_{t=0}^{t=t} \quad (\text{B.3})$$

or

$$c_t - c_0 = k_s (\rho O_2)^q t \quad (\text{B.4})$$

But, recall that

$$c = \frac{1}{M_n} \quad (\text{B.5})$$

where M_n is the number-average molecular weight. Then,

$$\frac{1}{M_{n_t}} - \frac{1}{M_{n_0}} = k_s (\rho O_2)^q t \quad (\text{B.6})$$

Equation (B.6) is useful but does not allow the assessment of shear on the reaction rate; to arrive at a useful expression, let

$$k_s = A'_s \exp(-E_A/RT) \quad (\text{B.7})$$

where A'_s is the Arrhenius preexponential factor; E_{As} , the activation energy of chain-scission; R , a gas constant; and T , temperature, and let

$$A'_s = A_s \tau^m \quad (\text{B.8})$$

where A_s is the nonshear component of the preexponential factor; τ , the shear stress; and m , a constant; and $A_s \tau$ indicates that the probability of reaction is affected by shear.

Substituting eqs. (B.7) and (B.8) into eq. (B.6) yields

$$\left(\frac{1}{M_{n_t}} - \frac{1}{M_{n_0}} \right) = A_s \tau^m \exp(-E_{As}/RT) (\rho O_2)^q t \quad (\text{B.9})$$

Let

$$\left(\frac{1}{M_{n_t}} - \frac{1}{M_{n_0}} \right) \cdot \frac{1}{t} = NRCS = k_s \quad (\text{B.10})$$

where $NRCS$ = number-average rate of chain-scission (k_s).

Rearranging eq. (B.10) yields

$$\left(\frac{M_{n_0} - M_{n_t}}{M_{n_0} M_{n_t}} \right) \cdot \frac{1}{t} = NRCS \quad (\text{B.11})$$

Then,

$$NRCS = A_s \tau^m \exp(-E_{As}/RT) (\rho O_2)^q \quad (\text{B.12})$$

Equation (B.12) is unwieldy and does not clearly show all temperature dependencies. To obtain an expression that does, recall

$$\tau = \eta \dot{\gamma} \quad (\text{B.13})$$

where η is the polymer melt viscosity, and $\dot{\gamma}$, the shear rate. Substituting eq. (B.13) into eq. (B.12) and taking the ln of the expression yields

$$\ln(NRCS) = \ln A_s + m \ln \eta_t + m \ln \dot{\gamma}_t - \frac{E_{As}}{RT} + q \ln(\rho O_2) \quad (\text{B.14})$$

Recall also that

$$\eta_T = C_1 M_w^r \quad (\text{B.15})$$

where η_T is the viscosity at constant temperature; C_1 , a constant; M_w , the weight-average molecular weight; r , a constant, and

$$\eta_{M_w} = C_2 \exp(E_F/RT) \quad (\text{B.16})$$

where η_{M_w} is the viscosity at constant molecular weight; C_2 , a constant at $\dot{\gamma} = \text{constant}$; and E_F , the activation energy of flow.

Equations (B.15) and (B.16) are special cases of

$$\eta = C_{\dot{\gamma}} M_w^r \exp(E_F/RT) \quad (\text{B.17})$$

where $C_{\dot{\gamma}}$ is a constant at constant $\dot{\gamma}$. Then, substituting into eq. (B.14) yields

$$\ln(NRCS) = \ln A_s + m \ln C_{\dot{\gamma}} + mr \ln M_{w_t} + \frac{mE_F}{RT} + m \ln \dot{\gamma}_t - \frac{E_{As}}{RT} + q \ln(\rho O_2) \quad (\text{B.18})$$

or

$$\ln(NRCS) = \left(\frac{mE_F - E_{As}}{RT} \right) + m \ln \dot{\gamma}_t + mr \ln M_{w_t} + \ln A_s + m \ln C_{\dot{\gamma}} + q \ln(\rho O_2) \quad (\text{B.19})$$

*Assume at low degrees of chain-scission that

$$\ln M_{w_t} \simeq \ln M_{w_0} \quad (\text{B.20})$$

Then, eq. (B.19) becomes

$$\ln(NRCS) \simeq \left(\frac{mE_F - E_{As}}{RT} \right) + m \ln \dot{\gamma}_t + mr \ln M_{w_0} + \ln A + m \ln C_{\dot{\gamma}} + q \ln(\rho O_2) \quad (\text{B.21})$$

Then, at $\dot{\gamma}_t = \text{constant} = \dot{\gamma}$, $C_{\dot{\gamma}} = \text{constant}$, and

$$\ln(NRCS)_{\dot{\gamma}} \simeq \left(\frac{mE_F - E_{As}}{RT} \right) + \text{constant} \quad (\text{B.22})$$

and

$$\Delta \ln(NRCS)_{\dot{\gamma}} / \Delta(1/T) \simeq \left(\frac{mE_F - E_{As}}{R} \right) \quad (\text{B.23})$$

Equations (B.22) and (B.23) allow the assessment of activation energy functionality from number-average molecular weight data. To use weight-average molecular weight data, it is necessary to modify these equations.

Consider eq. (B.10), where

$$\left(\frac{1}{M_{n_t}} - \frac{1}{M_{n_0}} \right) \cdot \frac{1}{t} = NRCS \quad (\text{B.10})$$

Recall that

$$\frac{M_w}{M_n} = PD \quad (\text{B.24})$$

where M_w is the weight-average molecular weight, and PD , the polydispersity. Substituting into eq. (B.10) yields

$$\left(\frac{PD}{M_{w_t}} - \frac{PD}{M_{w_0}}\right) \cdot \frac{1}{t} = NRCS \quad (\text{B.25})$$

or

$$\left(\frac{1}{M_{w_t}} - \frac{1}{M_{w_0}}\right) \cdot \frac{PD}{t} = NRCS \quad (\text{B.26})$$

Combining with eq. (B.10) yields

$$\left(\frac{1}{M_{n_t}} - \frac{1}{M_{n_0}}\right) \cdot \frac{1}{t} = \left(\frac{1}{M_{w_t}} - \frac{1}{M_{w_0}}\right) \cdot \frac{PD}{t} \quad (\text{B.27})$$

Let

$$\left(\frac{1}{M_{w_t}} - \frac{1}{M_{w_0}}\right) \cdot \frac{1}{t} = WRCS = k'_s \quad (\text{B.28})$$

where $WRCS$ is the weight-average rate of chain scission (k'_s). Then,

$$NRCS = WRCS \cdot PD \quad (\text{B.29})$$

or

$$\ln(NRCS) = \ln(WRCS) + \ln PD \quad (\text{B.30})$$

This relationship allows weight-average molecular weight data to be used with number-average molecular weight data.

To obtain a value for m , consider eq. (B.12). For resin A , at $T = \text{constant}$,

$$\ln NRCS_{A,T} = \ln A_s + m \ln \tau_{A,t,T} - \frac{E_{As}}{RT} + q \ln(\rho O_2) \quad (\text{B.31})$$

For resin B , at $T = \text{constant}$,

$$\ln NRCS_{B,T} = \ln A_s + m \ln \tau_{B,t,T} - \frac{E_{Bs}}{RT} + q \ln(\rho O_2) \quad (\text{B.32})$$

Then, subtracting eq. (B.32) from (B.31) yields

$$\ln NRCS_{A,T} - \ln NRCS_{B,T} = m \ln \tau_{A,t,T} - m \ln \tau_{B,t,T} \quad (\text{B.33})$$

or

$$\frac{[\ln NRCS_{A,T} - \ln NRCS_{B,T}]}{\div [\ln \tau_{A,t,T} - \ln \tau_{B,t,T}]} = m \quad (\text{B.34})$$

or

$$\frac{[\ln NRCS_{A,T} - \ln NRCS_{B,T}]}{\div [\ln \text{Torq}_{A,t,T} - \ln \text{Torq}_{B,t,T}]} = m \quad (\text{B.35})$$

allowing the determination of m .

Where for a Brabender Plasti-Corder

$$\tau = C_3 \text{Torq} \quad (\text{B.36})$$

and where C_3 is a constant, dependent on bowls and blades, and Torq is the Brabender torque.

Let

$$\text{Torq}_{A,t,T} = \text{Torq}_{m,A,T} \quad (\text{B.37})$$

and

$$\text{Torq}_{B,t,T} = \text{Torq}_{m,B,T} \quad (\text{B.38})$$

where $\text{Torq}_{m,T}$ is the minimum Brabender torque, the torque at the onset of cross-linking at $T = \text{constant}$. Then, at $\dot{\gamma} = \text{constant}$,

$$\frac{[\ln NRCS_{A,T,\dot{\gamma}} - \ln NRCS_{B,T,\dot{\gamma}}]}{\div [\ln \text{Torq}_{m,A,T,\dot{\gamma}} - \ln \text{Torq}_{m,B,T,\dot{\gamma}}]} \simeq m \quad (\text{B.39})$$

This expression also allows the determination of m ; to obtain a value of mr , consider, also, eq. (B.21) for resins A and B at constant T and $\dot{\gamma}$. Then,

$$\frac{[\ln NRCS_{A,T,\dot{\gamma}} - \ln NRCS_{B,T,\dot{\gamma}}]}{\div [\ln M_{w_0,A} - \ln M_{w_0,B}]} \simeq mr \quad (\text{B.40})$$

From eq. (B.40), a value of mr can be determined.

A value of r can be determined from eq. (B.15), re-written at constant $\dot{\gamma}$ as

$$\ln \eta_{T,\dot{\gamma}} = \ln C_1 + r \ln M_w \quad (\text{B.41})$$

REFERENCES

1. P. T. DeLassus, G. Strandburg, and B. A. Howell, *Tappi J.*, **71**, 177 (1988) and references cited therein.
2. R. A. Wessling, D. S. Gibbs, P. T. DeLassus, and B. A. Howell, in *Encyclopedia of Polymer Science and Engineering*, 2nd ed., Vol. 17, Wiley, New York, 1989, pp. 492 ff.

3. B. A. Howell, *J. Polym. Sci. Polym. Chem. Ed.*, **25**, 1681 (1987).
4. B. A. Howell and P. T. DeLassus, *J. Polym. Sci. Polym. Chem. Ed.*, **25**, 1697 (1987).
5. B. A. Howell, A. M. Kelly-Rowley, and P. B. Smith, *J. Vinyl Tech.*, **11**, 159 (1989).
6. B. A. Howell, *Thermochim. Acta*, **134**, 207 (1988).
7. J. D. Danforth, *Polym. Prepr.*, **21**, 140 (1980).
8. S. N. Zhurkov and V. E. Korsukov, *J. Polym. Sci. Polym. Phys. Ed.*, **12**(2), 385 (1974).
9. N. M. Emanuel and A. L. Buchachenko, *Chemical Physics of Polymer Degradation and Stabilization*, VNU Science Press, Utrecht, The Netherlands, 1987, Chap. 8.
10. V. Ye. Korsukov, V. I. Vettegren, I. I. Novak, and L. P. Zaitseva, *Polym. Sci. U.S.S.R.*, **16**, 1781 (1974).
11. K. J. Laidler and J. H. Meiser, *Physical Chemistry*, Benjamin/Cummings, Menlo Park, CA, 1982, pp. 378-383.
12. H. A. Pohl and J. K. Lund, *Soc. Plast. Eng. Tech. Pap.*, **5**, 7-1 (1959).
13. H. A. Pohl and C. G. Gogos, *J. Appl. Polym. Sci.*, **5**, 67 (1961).
14. R. A. Wessling, D. S. Gibbs, P. T. DeLassus, and B. A. Howell, in *Encyclopedia of Polymer Science and Engineering*, 2nd ed., Vol. 17, Wiley, New York, 1989, pp. 511-516.
15. R. T. Conley and P. L. Valint, *J. Appl. Polym. Sci.*, **9**, 785 (1965).
16. J. E. Goodrich and R. S. Porter, *Polym. Eng. and Sci.*, **45** (1967).
17. B. A. Howell and P. B. Smith, *J. Polym. Sci. Polym. Phys. Ed.*, **26**, 1287 (1988).
18. V. V. Lisitskii, A. P. Savel'ev, V. I. Manushin, and K. S. Minsker, *Int. Polym. Sci. Tech.*, **8**(7), T/45 (1981).
19. T. Kelen, *Polymer Degradation*, Van Nostrand Reinhold, New York, 1983, pp. 96-102.
20. R. A. Wessling, *Polyvinylidene Chloride*, Gordon and Breach, New York, 1977.
21. T. H. Lowry and K. S. Richardson, *Mechanism and Theory in Organic Chemistry*, Harper & Row, New York, 1987, pp. 919-926.
22. J. Wypych, *Polyvinyl Chloride Degradation*, Elsevier, New York, 1985, pp. 43-47.
23. K. B. Abbas and E. M. Sorvik, *J. Appl. Polym. Sci.*, **19**, 2991 (1975).
24. K. B. Abbas and E. M. Sorvik, *J. Appl. Polym. Sci.*, **17**, 3577 (1973).

Received September 4, 1992

Accepted June 7, 1993